Microplastics: What happens in the human digestive tract? First evidences in adults using in vitro gut models

Elora Fournier, Mathilde Leveque, Philippe Ruiz, jérémy ratel, Claude Durif, Sandrine Chalancon, Frederic Amiard, Mathieu E Edely, Valérie Bézirard, Eric Gaultier, et al.

Journal of Hazardous Materials 442 (2023) 130010

Contents lists available at ScienceDirect

Journal of Hazardous Materials

journal homepage: www.elsevier.com/locate/jhazmat

Microplastics: What happens in the human digestive tract? First evidences in adults using in vitro gut models

Elora Fournier [a,b], Mathilde Leveque [b], Philippe Ruiz [a], Jeremy Ratel [c], Claude Durif [a], Sandrine Chalancon [a], Frederic Amiard [d], Mathieu Edely [d], Valerie Bezirard [b], Eric Gaultier [b], Bruno Lamas [b], Eric Houdeau [b], Fabienne Lagarde [d], Erwan Engel [c], Lucie Etienne-Mesmin [a], Stéphanie Blanquet-Diot [a,*,1], Muriel Mercier-Bonin [b,**,1]

[a] Université Clermont Auvergne, INRAE, UMR 454 MEDIS, F-63000 Clermont-Ferrand, France
[b] Toxalim, Research Centre in Food Toxicology, INRAE, ENVT, INP-Purpan, UPS, Université de Toulouse, F-31000 Toulouse, France
[c] INRAE, UR QuaPA, F-63122 Saint-Genès-Champanelle, France
[d] Le Mans Université, IMMM UMR-CNRS 6283, Avenue Olivier Messiaen, F-72085, Le Mans Cedex 9, France

HIGHLIGHTS

- Repeated exposure to PE MPs induced adult donor-dependent effects in M-ARCOL.
- The composition of the human gut microbiota was affected by repeated exposure to PE MPs.
- Common or distinct effects were observed between luminal and mucosal gut microbiota.
- Production of indole, 3-methyl-(skatole) increased after repeated exposure to PE MPs.

GRAPHICAL ABSTRACT

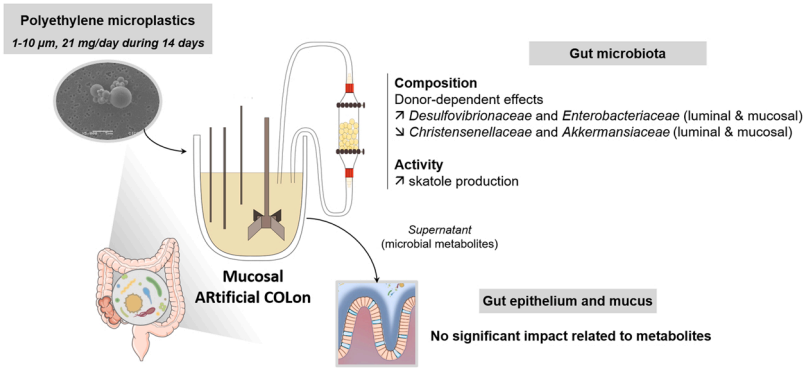

ARTICLE INFO

Editor: R. Teresa

ABSTRACT

Microplastics (MPs) are ubiquitous in the environment and humans are inevitably exposed to them. However, the effects of MPs in the human digestive environment are largely unknown. The aim of our study was to investigate the impact of repeated exposure to polyethylene (PE) MPs on the human gut microbiota and intestinal barrier

Abbreviation: AhR, aryl hydrocarbon receptor; ASV, amplicon sequence variant; DSC, differential scanning calorimetry; GAPDH, glyceraldehyde-3-phosphate dehydrogenase; GC-MS, gas chromatography-mass spectrometry; HRP, horseradish peroxydase; IL-8, interleukin-8; LDPE, low density polyethylene; LY, lucifer yellow; MP, microplastic; MUC2, mucin 2; MUC5AC, mucin 5AC; M-ARCOL, mucosal artificial colon; OCLN, occludin; Papp, apparent permeability coefficient; PE, polyethylene; qPCR, quantitative polymerase chain reaction; SCFA, short chain fatty acid; SPME, solid-phase microextraction; TEER, trans-epithelial electrical resistance; TGA, thermogravimetric analysis; VOC, volatile organic compound; ZO-1, zonula occludens-1.

* Corresponding author at: INRAE, UMR 454 MEDIS, 28 place Henri Dunant, 63000 Clermont-FD, France.
** Corresponding author at: Toxalim, UMR INRAE 1331, 180 chemin de Tournefeuille, BP 93173, 31027 Toulouse cedex 3, France.
E-mail addresses: stephanie.blanquet@uca.fr (S. Blanquet-Diot), muriel.mercier-bonin@inrae.fr (M. Mercier-Bonin).
[1] co-senior authors.

https://doi.org/10.1016/j.jhazmat.2022.130010
Received 1 August 2022; Received in revised form 8 September 2022; Accepted 15 September 2022
Available online 21 September 2022

Keywords:
Microplastics
Polyethylene
Gut microbiota
in vitro gut model
Intestinal cell model

using, under adult conditions, the Mucosal Artificial Colon (M-ARCOL) model, coupled with a co-culture of intestinal epithelial and mucus-secreting cells. The composition of the luminal and mucosal gut microbiota was determined by 16S metabarcoding and microbial activities were characterized by gas, short chain fatty acid, volatolomic and AhR activity analyses. Gut barrier integrity was assessed via intestinal permeability, inflammation and mucin synthesis. First, exposure to PE MPs induced donor-dependent effects. Second, an increase in abundances of potentially harmful pathobionts, *Desulfovibrionaceae* and *Enterobacteriaceae*, and a decrease in beneficial bacteria such as *Christensenellaceae* and *Akkermansiaceae* were observed. These bacterial shifts were associated with changes in volatile organic compounds profiles, notably characterized by increased indole 3-methyl- production. Finally, no significant impact of PE MPs mediated by changes in gut microbial metabolites was reported on the intestinal barrier. Given these adverse effects of repeated ingestion of PE MPs on the human gut microbiota, studying at-risk populations like infants would be a valuable advance.

1. Introduction

While plastics were described as a revolutionary material in the 1950s, they have increasingly become a global environmental threat affecting all ecosystems (Wang et al., 2021; Su et al., 2022). In the environment, plastic debris undergo a progressive weathering, releasing smaller plastic particles (Zhang et al., 2021a). In their attempt to reach a consensus on the definition of microplastics (MPs) that incorporates all the most important characteristics, Frias and Nash (2019) defined them as any synthetic solid particles or polymeric matrices, with regular or irregular shape and with size ranging from 1 μm to 5 mm, of either primary (i.e. voluntarily manufactured) or secondary (i.e. released from plastic debris weathering and fragmentation) manufacturing origin, which are insoluble in water (Frias and Nash, 2019). Many types of plastic types are produced worldwide, but the most prevalent polymer is polyethylene (PE) (Anon, 2021).

The deleterious consequences on the environment and organisms resulting from plastic pollution are now well established (Bucci et al., 2019). Inevitably, MPs enter the food chain, with converging studies reporting their presence in drinking water and several foods (Fournier et al., 2020). This has raised concern about the potential health effects of MPs after ingestion (Lehel and Murphy, 2021; Provencher et al., 2020), since their presence has been assessed in human blood (Leslie et al., 2022), colonic tissues (Ibrahim et al., 2021) and stools (Zhang et al., 2021a, 2021a; Schwabl et al., 2019). However, assessing the health risk of MPs in humans remains a global challenge to date. In particular, little is known about the fate of these particles in the human digestive tract. During their transit, MPs encounter the gut barrier composed, in its luminal side, of intestinal epithelium and mucus and gut microbiota, which prevents the host from translocation of exogenous aggressors in the form of foreign particles and pathogens (Pelaseyed et al., 2014; Birchenough and Johansson, 2020). The mucus layer, a viscoelastic gel that lines and protects the intestinal epithelium, constitutes the first line of physical, chemical and biological defense of the host. Secreted by goblet cells, mucus is notably composed with complex glycoproteins, called mucins (MUC2 in the human intestine) (Etienne-Mesmin et al., 2019). The gut microbiota refers to this complex and diverse community of microbes from almost all kingdoms of life, composed of bacteria, viruses, fungi, archaea and protozoa harbored along the human gut and especially in the colon (Rooks and Garrett, 2016; Thursby and Juge, 2017). These microorganisms, coexisting and interacting in the gut, contribute to various essential functions for host physiology. For instance, they play a role in the regulation of host immunity but also in the participation in the metabolism of drugs, toxins and xenobiotics (Claus et al., 2016; Andoh, 2016; Lindell et al., 2022). In addition, they enable the breakdown of undigested food (e.g. dietary fibers), resulting in significant production of secondary metabolites, such as gas, short chain fatty acids (SCFAs) (Kalantar-Zadeh et al., 2019; Morrison and Preston, 2016), volatile organic compounds (VOCs) (Raman et al., 2013) and aryl hydrocarbon receptor (AhR) ligands mainly derived from tryptophan metabolisms (Lamas et al., 2018). In particular, SCFAs and AhR ligands are involved in the preservation of the integrity of intercellular tight junctions in the intestinal epithelium, thereby establishing the link between the gut microbial activity and the maintenance of effective intestinal barrier function. Thus, deciphering the potential interactions between MPs and the gut microbiota, as well as the intestinal mucus and epithelium, is a critical issue that has been little explored to date. Studies in rodents have shown a variety of effects of MPs, depending on particle size, polymer type, shape, surface charge, as well as duration of exposure, mode of administration and dose tested. These effects included altered mucus synthesis and secretion and dysbiosis of the microbiota, which could exacerbate diseases (Jin et al., 2019; Lu et al., 2018; Li et al., 2020; Djouina et al., 2022; Sun et al., 2021), accompanied by local inflammation, oxidative stress and metabolic disruption. Murine model investigations are still widely used in toxicological studies because they have physiological relevance to a certain extent. However, due to differences in rodent/human physiology and gut microbiota (Hugenholtz and de Vos, 2018) but also due to the incentive for in vitro approaches by the application of European 3R (Replacement, Refinement and Reduction) principle rules (Prescott and Lidster, 2017), dynamic in vitro colonic models mimicking the human physiological conditions, including gut microbiota, represent powerful alternative tools, which have been little explored for MPs (Fournier et al., 2021a). The main studies in the in vitro literature to date have focused on cell culture experiments simulating the epithelium/mucus barrier. As for in vivo studies, various impacts on cell cytotoxicity, permeability and inflammation have been described, depending on polymer type, particle size, concentration and surface properties (Gautam et al., 2022; Liu et al., 2020a; Stock et al., 2022; Zhang et al., 2021b). In this work, we focused on polyethylene (PE), one of the major manufactured polymers (Anon, 2021), and widely found in flexible and rigid packaging for food, but also cosmetics, medical or industrial applications. It is also the most abundant type of plastic polluting marine environments (Erni-Cassola et al., 2019). We hypothesized that exposure to PE MPs could affect the human adult digestive environment in vitro under realistic conditions (i.e. repeated exposure to a human-relevant dose with potential inter-individual variability). To address these questions, we investigated the impact of a 2-week daily exposure to PE MPs on the human gut microbiota composition and metabolic activity (production of gas, SCFAs and VOCs, AhR activation) in four healthy adult volunteers using the in vitro Mucosal Artificial Colon model (M-ARCOL). This model is a one-stage fermentation system, which simulates the mean physico-chemical and microbial parameters of the human colon, including not only the luminal but also mucosal microbiota through an external mucin-alginate beads compartment (Deschamps et al., 2020). Co-cultures of human Caco-2 and mucus-secreting HT29-MTX intestinal cells were then incubated with M-ARCOL luminal supernatants collected after the 2-week exposure period in order to decipher the potential effects on intestinal mucus and epithelium (cytotoxicity, permeability, inflammation).

2. Materials and methods

2.1. Characterization of MPs

PE microspheres (CPMS-0.96 1–10 μm - 0.2 g; non-fluorescent

particles) were purchased from Cospheric (USA). The initial powder was suspended (2.625 mg/mL) in a sterile deionized water solution with 0.01 % (w/v) Tween 80. Particle size was determined using the smile-view software from scanning electron microscopy images captured with the JSM 6060LV microscope (Jeol, Japan). To determine the polymeric composition, the powder was analyzed using differential scanning calorimetry (DSC) and thermogravimetric analysis (TGA). The DSC measurements were performed on a Mettler DSC3^{+} device (N.V. Mettler-Toledo S.A., Belgium). The equipment is calibrated with Indium. A few mg of material were placed into an aluminum pan and then subjected to a temperature cycle ranging from 25 °C to 200 °C under a nitrogen gas flow. A rate of 10 °C/min was applied to heat and cool the material during the experiment. TGA measurements were performed on a Mettler TGA2 device (N.V. Mettler-Toledo S.A., Belgium). The analysis was

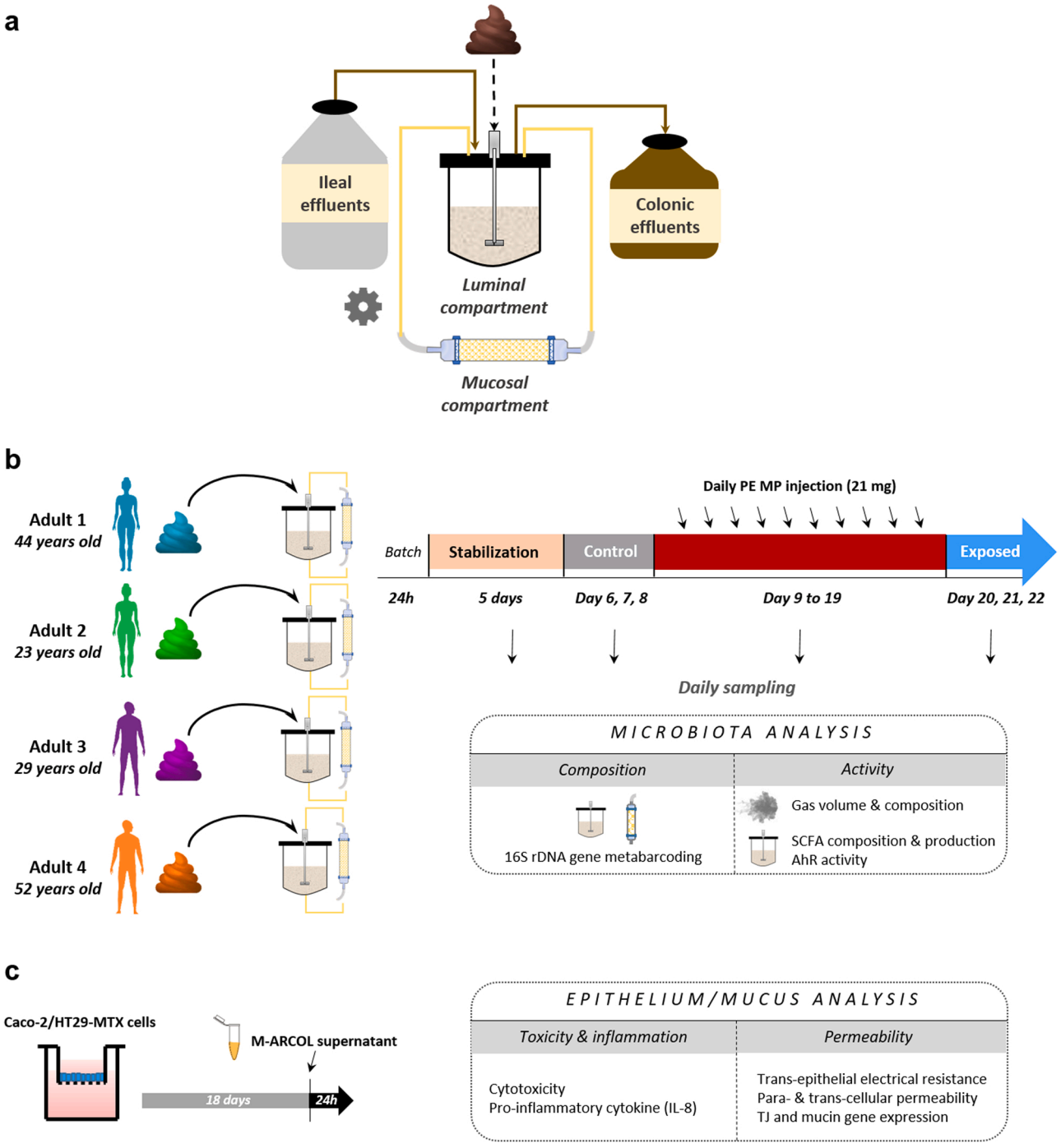

Fig. 1. Outline of in vitro fermentation in M-ARCOL and Caco-2/HT29-MTX cell culture experiments. a) Schematic representation of the M-ARCOL colonic model. b) M-ARCOL experimental design and analysis. Four bioreactors inoculated with fecal samples from four different adults were run in parallel. After an 8-day stabilization phase, PE MPs were added daily into the bioreactor tank at a concentration of 21 mg for 14 days. The last three days of the stabilization period were chosen as control days ('control', day 6, 7, 8) while the last three days of the exposure period were selected as exposure days ('exposed', day 20, 21, 22). Gas and luminal fermentation medium were sampled daily while mucin-alginate beads were collected every other day for further analysis of gut microbiota structure and activity. c) Cell culture experimental design and analysis. Caco-2 and HT29-MTX intestinal cells in co-culture (90/10) were seeded using inserts. After an 18-day cell growth period, cells were exposed during 24 h to day 8 or day 22 luminal supernatants of M-ARCOL and cytotoxicity, inflammation, intestinal permeability and mucin synthesis were evaluated. *AhR: aryl hydrocarbon receptor; IL-8: interleukin-8; MP: microplastic; PE: polyethylene; SCFA: short chain fatty acid; TJ: tight junction.*

performed at a heating rate of 10 °C/min under a nitrogen gas flow up to 800 °C.

2.2. Fecal sample collection and treatment

Donors were selected according to their sex (two males, two females), their age (age range between 23 and 52 years old) and their dietary habits (flexitarian and western like diet). All selected donors had no history of antibiotic treatment, drug or probiotic consumption for 3 months prior to sample collection.

Immediately after defecation, the fecal samples were transferred to a sterile container placed in an airtight anaerobic box (GENbag anaer gas pack systems, Biomerieux, France) and transported at ambient temperature. They were then processed at the laboratory within 6 h after defecation. In an anaerobic chamber (COY laboratories, USA), 11 g of each fresh stool sample were suspended in 110 mL of 30 mM sterile sodium phosphate buffer and filtered (500 μm stainless steel sieve).

2.3. Description and set-up of the M-ARCOL model

The Mucosal Artificial Colon (M-ARCOL) is a one-stage fermentation system (MiniBio, Applikon, The Netherlands), operated under continuous conditions, which simulates the physico-chemical and microbial conditions (both luminal and mucosal environments) encountered in the adult colon (Deschamps et al., 2020; Thévenot et al., 2015). The operating parameters (temperature, pH, retention time, volume, stirring speed) as well as the composition of the nutritive medium are given in Table S1. The M-ARCOL model is composed of a main bioreactor (luminal compartment) connected to an external glass compartment (mucosal compartment) containing mucin-alginate beads (Fig. 1a). These beads were prepared with mucin from porcine stomach type II (Sigma-Aldrich, USA) and sodium alginate (Sigma-Aldrich, USA), as previously described (Deschamps et al., 2020). The beads were stored at 4 °C before introduction into the hermetically sealed glass compartment (total beads area 556 cm^2) connected to the bioreactor. M-ARCOL was set-up, based on in vivo data, to reproduce the average conditions found in the colon of a healthy human adult and the nutritive medium was adapted to mimic the composition of ileal effluents, based on previous studies (Deschamps et al., 2020; Thévenot et al., 2015) (Fig. 1a). The temperature was maintained at 37 °C, the average retention time was set at 24 h and the pH was maintained at a constant value of 6.3 by addition of 2 M NaOH. After an initial N_2 flush upon introduction of the fecal inoculum, anaerobiosis was maintained inside the bioreactor by the activity of the resident microbiota alone, to mimic as closely as possible the in vivo situation. Mucin-alginate beads were renewed every 2 days while maintaining the external compartment under anaerobiosis through a constant flow of CO_2.

2.4. Experimental design and sampling in M-ARCOL

The experimental design and sampling are shown in Fig. 1b. Four M-ARCOL bioreactors were inoculated with fecal samples from four adult donors and operated in parallel. Fermentations were performed under continuous conditions for 22 days, after a 24-h batch microbial amplification. An 8-day microbiota stabilization phase was applied and the three last days of this period (i.e. days 6, 7 and 8) were chosen as 'control days'. Subsequently, to mimic human chronic exposure, 14 days of daily exposure to PE MPs (21 mg of MPs in 8 mL of a deionized water solution containing 0.01 % (w/v) Tween 80) were performed and the three last days (i.e. days 20, 21 and 22) were selected as 'exposed days'. Samples from the main bioreactors, termed luminal microbiota, were collected daily for microbiome characterization (storage at −80 °C) and SCFA analysis (storage at −20 °C). Additional samples from the mucin bead compartment, termed mucosal microbiota, were collected every 2 days (when the mucin-alginate beads were replaced) for microbiota characterization. The beads were washed twice in sterile phosphate buffer saline -PBS- (pH 7.1) and stored at −80 °C before downstream analyses. The medium surrounding the mucin-alginate beads was also collected at the same time. Additional luminal samples were collected at day 8 (control) and day 22 (exposure) for cell culture experiments, scanning electron microscopy, and volatolomic analysis. Samples were also collected daily from the atmospheric phase of the bioreactors to verify anaerobic conditions and determine gas composition. The daily extra volume of gas produced by microbial fermentation was also measured using a syringe connected to the gas bag.

2.5. Extraction of DNA

Genomic DNA was extracted from luminal and mucosal samples using the QIAamp Fast DNA Stool Mini Kit (12830–50, Qiagen, Germany) following the manufacturer's instructions with the following adjustments. Prior to DNA extraction, luminal samples were centrifuged (2000 g, 10 min, 4 °C) and the pellet was mechanically disrupted using a bead beater (5 min, 20 beat/sec) with 300 mg of sterile glass beads (diameter ranging from 0.1 to 0.6 mm), incubated (70 °C, 5 min) and centrifuged (12,000 g, 1 min, 4 °C). Mucosal samples were subjected to the following modifications prior to DNA extraction: 10 min of incubation with citrate buffer (37 °C), as previously described (Capone et al., 2013), before vortexing (maximal speed, 3 min) and centrifugation (8000 g, 1 min). DNA integrity was verified by agarose gel electrophoresis and by Nanodrop 2000 analysis (Thermo Fisher Scientific, USA). The DNA quantity was assessed using the Qubit dsDNA Broad Range Assay Kit (Q32851, Invitrogen, USA) with a Qubit 2.0 Fluorometer (Invitrogen, USA). Samples were stored at − 20 °C before microbiota analysis (qPCR and 16S metabarcoding).

2.6. Total bacteria quantification by qPCR

Total bacteria were quantified by qPCR using primers BAC338R and BAC516F with hybridization temperature set at 58 °C (Yu et al., 2005) (Table S2). Real-time PCR assays were performed on a Biorad CFX96TM Real-Time System (Bio-Rad Laboratories, USA) using the Takyon™ Low Rox SYBR® 2X MasterMix blue dTTP kit (B0701, Eurogentec, Belgium). Each reaction was run in duplicate in a final volume of 10 μL with 5 μL of Master Mix, 0.45 μL of each primer (10 μM), 1 μL of DNA sample (10 ng/μL) and 3.1 μL of ultrapure water. Amplifications were performed as follows: 1 cycle at 95 °C for 5 min, followed by 40 cycles at 95 °C for 30 s and 60 °C for 1 min. A melting step was added to ensure primer specificity. The standard curve was generated from 10-fold dilutions of bacterial DNA (extracted from a fermentation sample), allowing the calculation of DNA concentrations as described in (Deschamps et al., 2020).

2.7. 16S metabarcoding and data analysis

The bacterial V3-V4 region of the 16S ribosomal DNA (rDNA) was amplified with primers V3_F357_N and V4_R805 for the bacterial fraction and Arch349F and Arch806R for the methanogenic Archaea. Amplicons were generated using a Fluidigm Access Array followed by high-throughput sequencing on an Illumina MiSeq system performed at the Carver Biotechnology Center of the University of Illinois (Urbana, USA).

Bioinformatics analysis was performed by GeT-Biopuces platform (INSA/Toulouse Biotechnology Institute, Toulouse, France) with R software version 4.1.1 (2021–08–10) and rANOMALY package (Theil and Rifa, 2021). The demultiplexed raw sequence data were filtered by quality and the denoising process was performed using DADA2 version 1.20.0 (Callahan et al., 2016). Reads with N bases or low phred quality score (under 2) were eliminated and reads under 100 pb length were removed. Decontamination steps were performed to filter out sequences corresponding to PhiX DNA used as a spike-in control for MiSeq runs and chimeric sequences were filtered out. Taxonomic affiliation of all

amplicon sequence variants (ASVs) was performed with idtaxa function from DECIPHER package version 2.20.0 (Murali et al., 2018) using SILVA release 138 (Quast et al., 2013) and GTDB bac120_arc122 (Parks et al., 2022) databases (60 % bootstrap cut-off). To improve the completeness of taxonomic affiliation, alignments were carried out using BLAST (Altschul et al., 1990) (98 % identity and coverage) on representative sequences of unassigned ASVs or assigned with incomplete taxonomy. A phylogenetic tree was constructed based on the representative ASVs sequences using the functions of the phangorn package version 2.7.1 (Schliep et al., 2017). α- and β-diversity indexes were calculated using the diversity_alpha_fun function from rANOMALY package (Theil and Rifa, 2021). The diversity of the microbiota across the samples was described using a Bray-Curtis dissimilarity-based redundancy analysis (RDA) using vegan R-package version 2.5–7 (Oksanen et al., 2011). The impact of the different parameters studied (i.e. total gas and SCFA production, gas and SCFA composition, type of sample (luminal or mucosal), time and sex of donors) on the dissimilarities between the groups was evaluated using PERMANOVA permutation tests (999 permutations).

2.8. Gas analysis

The analysis of O_2, N_2, CO_2, CH_4 and H_2 produced during the fermentation process in the atmospheric phase of the main bioreactors was performed using a HP 6890 gas chromatograph (Agilent Technologies, USA) coupled with a micro-TCD detector (Agilent Technologies, USA) (Deschamps et al., 2020). Two series columns, Molecular Sieve 5A and Porapack Q (Agilent Technologies, USA), were used. Gas composition was determined using calibration curves made from ambient air (78.09 % N_2, 20.95 % O_2, 0.04 % CO_2) and 3 gas mixtures A (5 % CO_2, 5 % H_2, 90 % N_2), B (19.98 % CO_2, 80.02 % H_2) and C (19.89 % CO_2, 19.88 % CH_4, 20 % H_2, 40.23 % N_2).

2.9. Analysis of SCFAs

2 mL of each luminal sample was centrifuged (5000 g, 15 min, 4 °C) and 900 µL of supernatant was diluted at 1/10 in 0.04 M H_2SO_4 mobile phase, vortexed and filtered (pore size 0.22 µm). The three major SCFAs (acetate, propionate and butyrate) were quantified by high-performance liquid chromatography (HPLC) (Elite LaChrom, Merck HITACHI, USA) coupled to a DAD diode (Deschamps et al., 2020). The HPLC column (150 × 7.8 mm) contained a negatively charged sulfonic-grafted polystyrene divinylbenzene stationary phase and carried an eluent containing acidified water. Data were obtained and analyzed by the EZChrom Elite software at 204 and 205 nm. SCFA concentrations were calculated from calibration curves established from solutions of known increasing concentration of acetate, propionate and butyrate (0, 10, 25 and 40 mM).

2.10. Measurement of AhR activity

The aryl hydrocarbon receptor (AhR) activity of luminal M-ARCOL luminal supernatants (see sample preparation in Section 2.14) after exposure to PE MPs (day 22) compared to control conditions (day 8) was measured using a luciferase reporter assay method, as previously described (Lamas et al., 2016). Briefly, mouse hepatocellular carcinoma H1L1.1c2 cells, containing a stably integrated dioxin response element-driven firefly luciferase reporter plasmid pGudLuc1.1, were seeded into 96-well plates at 10^5 cells/well in minimum essential medium Eagle alpha modification (MEM-α) medium (with 10 % (v/v) heat-inactivated fetal calf serum -FCS-, 1 % (v/v) penicillin/streptomycin and 1 % (v/v) Geneticin G418) and cultured (37 °C, 5 % CO_2) 24 h before stimulation with M-ARCOL luminal supernatants. After incubation, the wells were washed with 100 µL PBS (pH 7.0), and 50 µL of Promega lysis buffer (pH 7.8) was added to each well. The plates were shaken for 1 h for cell lysis. After addition of 100 µL of luciferase reagent (Promega, France), luciferase activity was measured using a luminometer (Tecan, Switzerland). Experiments were performed in triplicate. All values were normalized, based on the cytotoxicity of the samples using the lactate dehydrogenase activity assay (Promega, USA).

2.11. Volatolomic analysis

Volatile organic compounds (VOCs) from control (day 8) and exposed (day 22) luminal samples were analyzed by solid-phase microextraction (SPME) coupled with gas chromatography-mass spectrometry (GC-MS), as previously described (Defois et al., 2017, 2018). Briefly, the day before analysis, 2.2 mL of a saturated NaCl solution (360 g/L) was added to each sample (0.8 mL). The mixture vials were closed under a flow of N_2, vortexed for homogenization, and thawed for 24 h at 4 °C. The following steps were then performed with an automated sampler (AOC-5000 Shimadzu, Japan): (i) preheating of the sample to 40 °C for 10 min in the shaker (500 rpm), (ii) SPME trapping (75 µm carboxen/polydimethylsiloxane, 23-gauge needle, Supelco, USA) of the VOCs for 30 min at 40 °C, and (iii) thermal desorption at 250 °C for 2 min in splitless mode in the GC inlet. Further VOC analysis was performed by GC/MS-full scan (GC2010, QP2010 +, Shimadzu, Japan). VOCs were injected in a DB-5MS capillary column (60 m × 0.32 mm × 1 µm, Agilent, USA) according to the GC-MS settings used by Defois and collaborators (Defois et al., 2017, 2018). Provisional identification of VOCs was performed on the basis of mass spectra, by comparison with mass spectral libraries (Wiley Registry 12th Edition / NIST 2020), and retention indices (RI), by comparison with published RI values and with those of our in-house database. The peak area of the tentatively identified compounds was determined for each of the targeted molecules using a mass fragment selected for its specificity and freedom from co-elution.

2.12. Scanning electron microscopy (SEM) analysis

Luminal and mucosal samples of adult 3, selected as having the most diverse bacterial community in the initial stool inoculum (see Section 3.2), were deposited on SEMPore filters (Jeol, Japan) and fixed for 12 h at 4 °C in 0.2 M sodium cacodylate buffer at pH 7.4 containing 4 % (w/v) paraformaldehyde and 2.5 % (v/v) glutaraldehyde. Filters were washed 10 min in sodium cacodylate buffer (0.2 M, pH 7.4) and post-fixed 1 h with 1 % (w/v) osmium tetroxide in the same buffer. The filters were then washed 20 min in distilled water. Dehydration by graded ethanol was performed from 25° to 100° (10 min each) and completed in hexamethyldisilazane (HMDS) for 10 min. Samples were mounted on stubs using adhesive carbon tabs and sputter-coated with gold-palladium (JFC-1300, JEOL, Japan). Analysis was carried out using a scanning electron microscope JSM-6060LV (Jeol, Japan) at 5 kV in high-vacuum mode.

2.13. Raman spectroscopy mapping

Raman spectroscopy mapping was performed using a Raman spectrometer (Alpha300R Apyron, Witec, Germany) equipped with a confocal microscope. Exposed luminal samples (day 22, adult 3) were vacuum filtered using Anodisc filter (pore size 0.2 µm, diameter 25 mm). The filters were excited with a Coherent sapphire laser (532 nm, laser power 10 mW) and the Raman spectra were recorded in backscattering configuration using a 50X objective (Zeiss, Germany) with a numerical aperture of 0.55 to achieve a theoretical spatial resolution of 590 nm in the focus plane. Single Raman spectra were recorded 10 times with an integration time of 1 s. For each filter, maps between 900 and 2500 spectra were recorded with a step of 1.33 µm and 2 µm, respectively. For each mapping, the recorded signal (Raman signal plus background) was integrated over a 20 cm^{-1} spectral range centered at 1294 cm^{-1} corresponding to the CH_2 twisting vibration band of PE. The signal value was then automatically transformed by the software in a

color scale (from black to bright yellow).

2.14. Intestinal cell lines and cell culture conditions

The human colon adenocarcinoma Caco-2 cell line was obtained from the European Collection of Cell Cultures (ECACC, UK) and used at passage 58–62. The mucus-secreting colon adenocarcinoma HT29-MTX cell line was kindly provided by Dr. Thécla Lesuffleur (INSERM Lille, France) and used at passage 10–16. Both cell lines were maintained with culture medium (Dulbecco/Vogt modified Eagle's minimal essential medium -DMEM- without phenol red and 4.5 g/L glucose), supplemented with 1 % (v/v) penicillin/streptomycin, 1 % (v/v) non-essential amino acids (NEAA), 1 % (v/v) Glutamax and 10 % (v/v) heat-inactivated fetal bovine serum (FBS) at 37 °C in a humidified atmosphere of 5 % CO_2/95 % air. The medium was changed every 2–3 days and cells were split upon 80 % of confluence using Tryple express. Intestinal cells (90 % Caco-2/10 % HT29-MTX) (Gillois et al., 2021) were seeded in 24-well inserts of 1-μm pore size (Millipore, Merck Millipore SAS, France) and maintained in the culture medium. Starting on day 17, the FBS in the culture medium was replaced with 1 % (v/v) Insulin Transferrin Selenium (ITS) to limit interference with the samples to be tested. After 18 days, Caco-2/HT29-MTX co-cultures were apically incubated for 24 h with luminal samples of M-ARCOL, collected on day 8 (control) and day 22 (exposed), centrifuged (5000 g, 15 min, 4 °C) and diluted 20-fold (Fig. 1**c**). Experiments were performed with 3 biological replicates, 5 technical replicates for the day 8 (control) and 6 technical replicates for the day 22 (exposed).

2.15. Cell viability

To determine the potential cytotoxic effect of M-ARCOL supernatant samples on Caco-2/HT29-MTX cells and to establish sub-toxic conditions for testing on inserts, different dilutions (1/2, 1/5, 1/10, 1/20, 1/30 and 1/50 in cell culture medium) were evaluated. Cell viability was tested in triplicate with CytoTox 96® non-radioactive cytotoxicity assay (Promega, France) after 24 h of exposure. In 96-well plates, 25 μL of apical supernatants of the cell culture was diluted in 25 μL of ITS, 1 % culture medium and mixed with 50 μL of substrate. The plates were then incubated for 15 min at room temperature in the dark. The reaction was stopped with 50 μL of stop solution (1 M CH_3COOH) and absorbance at 490 nm was read with a Spark spectrophotometer (Tecan, Switzerland).

2.16. Intestinal permeability

Starting on day 12, the transepithelial electrical resistance (TEER) was continuously monitored in real time using the CellZScope2 device (NanoAnalytics, Germany). In addition, after the 24-h contact time with the 20-fold diluted supernatants of M-ARCOL, the inserts were transferred into a new 24-well plate containing 1 mL of Hank's balanced salt solution -HBSS- (pH 7.7). Lucifer yellow -LY- (0.4 mg/mL, molecular weight 457 g/mol) and horseradish peroxydase -HRP- (0.4 mg/mL, molecular weight 44,000 g/mol) were dissolved in HBSS and added to the apical compartment. After 2 h at 37 °C under 5 % CO_2/95 % air atmosphere, samples were taken from the apical and basolateral compartments. For LY measurement, samples were analyzed in duplicate using a Spark multimode plate reader (Tecan, Switzerland). Excitation and emission wavelengths were 405 nm and 535 nm, respectively. Total HRP was determined by an ELISA assay. Briefly, 96-well flat-bottomed black plates (Greiner, Dutcher, France) were coated overnight at 4 °C with 50 μL of 10 μg/mL mouse polyclonal to HRP (Abcam, France) in PBS. Plates were blocked with PBS-1 % bovine serum albumin (BSA) prior to incubation with apical and basolateral samples collected from inserts. Rabbit polyclonal anti-HRP biotin (Abcam, France) was added at a concentration of 10 μg/mL before the addition of fluorescein-5-isothiocyanate (FITC) conjugated streptavidin (Becton Dickinson, France) for 20 min and the fluorescence intensity measured at 485 nm/525 nm using a Spark microplate reader (Tecan, Switzerland). The apparent permeability coefficient (Papp in cm/s) was determined by the following equation: Papp=Cb/(SxC0), where Cb represents the level of LY or HRP accumulated in the basolateral compartment after 2 h, S represents the membrane area (0.33 cm^2) and C0 is the initial concentration of the marker (0.4 mg/mL -LY- or - HRP) in the apical compartment.

2.17. Interleukin-8 (IL-8) level measurement

The apical and basolateral media from the co-cultures were collected after the contact time of 24-h with 20-fold diluted supernatants of M-ARCOL and stored at −20 °C until analysis. Interleukin-8 (IL-8) levels were measured using the Quantikine Human IL-8 ELISA kit (DY208–05, R&D Systems, USA). Briefly, in Maxisorp 96-well plates (Nunc, France), biotinylated Goat polyclonal anti IL-8 was added at a concentration of 10 ng/mL before adding HRP-conjugated streptavidin (Becton Dickinson, France) for 20 min. Absorbance intensity was measured at 450 nm and 540 nm using a Spark microplate reader (Tecan, Switzerland).

2.18. Intestinal gene expression

Total RNAs were extracted from cells for each insert using the All-Prep RNA Mini kit (Qiagen, France) according to the manufacturer's instructions. Quantity and quality of extracted RNA samples were monitored using Nanodrop (Nanophotometer Implen, Dutscher, France) and Bioanalyzer (Agilent Technologies, USA), respectively. RNAs were reverse transcribed using enzyme IScript reverse transcription supermix (Biorad, France). Sample concentration was adjusted to 50 ng/μL. 384-well plates were filled by an Agilent Bravo Automated Liquid Handling Platform (Agilent Technologies, France). All wells contained 5 μL of the following mix: 2.5 μL of IQ SYBR green Supermix (Biorad, France), 1.5 μL of each primer set and 1 μL of cDNA sample. Amplification was performed using a ViiA7 Real-Time PCR System (Applied Biosystems, ThermoFisher Scientific, France). Thermal cycling conditions were as follows: 3 min denaturation at 95 °C followed by 40 cycles at 95 °C for 15 s and 45 s at 60 °C, and a melting curve step. The primer sequences of the targeted genes (genes encoding tight junction (TJ) proteins (zonula occludens-1 -*ZO-1*-, occludin -*OCLN-*) and genes involved in mucin synthesis (mucin 2 -*MUC2*-, mucin 5AC -*MUC5AC*-) are listed in Table S2. Raw data that passed quality control were analyzed with LinRegPCR (version 2021.2) and then normalized against the expression of glyceraldehyde-3-phosphate dehydrogenase (*GAPDH*), a reference housekeeping gene.

2.19. Statistical analysis

Statistical analyses on gut microbiota activity (gas, SCFAs and AhR activity), α-diversity indexes (number of observed ASVs and Shannon index) from metabarcoding data, as well as results from cell culture experiments obtained in control (day 8) and exposed (day 22) groups were processed using GraphPad Prism software version 9.3.1 for Windows (GraphPad Software, USA). Data normal distribution was verified by combining Anderson-Darling, D'Agostino & Pearson, Shapiro-Wilk and Kolmogorov-Smirnov tests and homoscedasticity was checked using the Fisher test. Then, appropriate statistical analysis was applied (either one-way ANOVA, Kruskal-Wallis or Welch's tests) and significance was considered for $p < 0.05$. For gut microbiota results, differential analyses (DESeq2, metagenomeSeq, metacoder) were performed on ExploreMetabar software using rANOMALY package (Theil and Rifa, 2021; Rifa and Theil, 2021). Principal coordinate analysis (PCoA) of unweight UniFrac distances was performed and significance between groups was assessed with a permutational multivariate analysis of variance (PERMANOVA) using ADONIS (999 permutations) with non-parametric tests. Volatolomics data were processed using the

Statistica Software (v.13) (StatSoft, France). Student's t-tests ($p < 0.05$) were performed for the VOC abundances determined in control (day 8) and exposed (day 22) groups and principal component analyses (PCA) were performed on the discriminant VOCs selected to visualize the structure of the data.

3. Results

3.1. Characterization of PE MPs

It was observed that MPs were spherical in shape with 71 % of the total number included in the size range defined by the supplier (1–10 μm). Of these, 50 % were in the size range between 1 and 2 μm (Fig. S1a). The DSC scans obtained from the heat of the initial MP powder showed an endothermic peak characteristic of melting of a PE material (Fig. S1b). The temperature at the maximum of the peak was measured to be about 112 °C, which is more relevant for a low-density PE (LDPE). Upon cooling of the material from its melting state, the crystallization peak appeared with a defined onset temperature of about 103 °C. No other effect could be observed in the temperature range studied. The thermal decomposition of the material was then analyzed by TGA (Fig. S1c). Only one weight loss was observed with a maximum of the degradation rate measured at approximately 467 °C. The decomposition was complete, 100 % of the material was lost during decomposition. Overall, these results confirmed that MPs were composed of pure PE polymer.

3.2. Characterization of initial human stool microbiota

A total of 199, 176, 205 and 140 ASVs were observed for adults 1, 2, 3 and 4, respectively, associated with the following Shannon indexes: 4.01, 3.97, 4.04 and 3.66 (data not shown). In addition, qPCR analysis revealed 3.88×10^9, 9.39×10^8, 4.38×10^9 and 6.02×10^9 16S rDNA gene copies/g of sample for adults 1, 2, 3 and 4, respectively (Fig. S2a). Regarding archaea, only *Methanobrevibacter* were detected with sequences number equal to 599, 1254, 3006 and 0 for adults 1, 2, 3 and 4, respectively. Only in adult 3, 4 sequences of *Methanomassiliicoccus* were also observed (Fig. S2b). At the phylum level, relative abundance profiles were donor-dependent but harbored mainly *Bacteroidota*, *Firmicutes*, *Verrucomicrobia* and *Proteobacteria* (Fig. S3a). The most significant differences between donors were observed in family abundance (Fig. S3b). While *Bacteroidaceae*, *Lachnospiraceae*, *Ruminococcaceae*, *Veillonellaceae*, *Akkermansiaceae* and *Rikenellaceae* were predominant, some family populations were specific to each donor. For instance, while adult 1 exhibited *Acidaminococcaceae*, adult 2 harbored *Prevotellaceae*, *Sutterellaceae* and *Clostridia UCG-017* family; adult 3, which had the most diverse inoculum, had *Christensenellaceae*, *Acutalibacteraceae*, *Prevotellaceae* and *Clostridia UCG-014* family. Finally, adult 4, which had the least diverse inoculum, was unremarkable despite the presence of *Clostridia UCG-014* family.

3.3. Bidirectional relationships between PE MPs and human gut microbiota during repeated exposure in M-ARCOL

3.3.1. Impact of exposure to PE MPs on the human gut microbiota composition

As shown in Fig. S2a, the total bacteria level was constant throughout the total duration of fermentation for both the lumen ($1.04 \times 10^{10} \pm 1.09 \times 10^9$, $3.40 \times 10^9 \pm 8.73 \times 10^8$, $7.07 \times 10^9 \pm 7.99 \times 10^8$, $9.96 \times 10^9 \pm 1.01 \times 10^9$ 16S rDNA gene copies/g of sample for adults 1, 2, 3 and 4, respectively) and mucus-associated ($4.78 \times 10^8 \pm 2.08 \times 10^8$, $3.83 \times 10^8 \pm 1.19 \times 10^8$, $8.61 \times 10^8 \pm 2.80 \times 10^8$, $8.35 \times 10^8 \pm 3.05 \times 10^8$ 16S rDNA gene copies/g of sample for adults 1, 2, 3 and 4, respectively) microbiota. The number of *Methanobrevibacter* sequences fluctuated during the fermentation and did not stabilize during the control period (Fig. S2b). However, archaeal populations were maintained over the 22-day period. From day 14, *Methanobrevibacter* sequences were detected in adult 4 in the luminal and mucosal compartments while none were reported in the inoculum.

Regarding the gut bacterial communities, the same major phyla of the initial inoculum were encountered but with different relative abundances, in a donor-dependent manner (Fig. S4a). This donor-dependent effect can be illustrated by the two-dimensional PCoA plot, based on the unweighted UniFrac distance matrix, over the days preceding exposure (stabilization phase including control days) (Fig. S4b). Clustering is highlighted according to the different donors for luminal and mucosal microbiota. For the control period (days 6, 7, 8), the profiles at the phylum level stabilized, with only minor variations in the observed relative abundance. With respect to the impact of exposure to PE MPs, no striking differences in exposed and non-exposed microbiota were notable at this taxonomic level.

At the family level (Fig. 2a), the donor effect remained noticeable and the relative abundance of families differed by donor. Interestingly, the impact of exposure to PE MPs was more striking at this taxonomic level. In particular, the results of the differential analysis at the family level, considering the mean of the data obtained for the four individuals (Fig. 2b), notably showed an increase in *Dethiosulfovibrionaceae* ($p < 0.005$), *Enterobacteriaceae* ($p < 0.0001$), *Desulfovibrionaceae* ($p < 0.005$) after exposure to PE MPs for luminal and mucosal microbiota. Of note, a significant increase in *Desulfovibrionaceae* due to exposure to PE MPs was observed for each of the four donors, whereas an increase in *Enterobacteriaceae* was found for three donors (adults 1, 3 and 4) in the luminal compartment (Fig. S5). In the mucosal compartment, a significant decrease in *Christensenellaceae* and *Akkermansiaceae* was observed for two donors (adults 3 and 4).

Regarding the diversity of the gut microbiota, exposure to PE MPs did not significantly impact the bacterial α-diversity indexes for luminal (Fig. 3a) and mucosal (Fig. 3b) microbiota. However, the number of observed ASVs tended to decrease after exposure in the microbiota of adults 1 and 2 while it slightly increased for adults 3 and 4. Representation of β-diversity by a two-dimensional PCoA plot, based on the unweighted UniFrac distance matrix between control and exposed days for luminal and mucosal microbiota, revealed a clear distinction for adults 3 and 4 (Fig. 3c).

3.3.2. Influence of the human gut microbiota on the surface properties of PE MPs

Conversely, we investigated the influence of the gut microbiota on the surface properties of PE MPs. To this end, luminal and mucosal samples from adult 3 before (day 8) and after exposure (day 22) were first analyzed by SEM (Fig. 4a). For the control conditions, as expected, a huge amount of microorganisms of various morphologies (bacilli, cocci and coccobacilli) were present in the luminal compartment but also some bacillus-like bacteria were observed on the surface of the mucin-alginate beads. For the exposed conditions, considering both luminal and mucosal samples, bacteria were in close contact with PE MPs. Furthermore, in order to decipher potential physico-chemical modifications of the PE MP surface due to these interactions, luminal samples were analyzed by Raman spectroscopy (Fig. 4b). The Raman spectrum of MPs in the luminal medium after exposure was identical to that obtained from the PE particles present in the initial suspension, showing that contact with the gut microbiota during fermentation does not induce major changes in the polymeric surface composition of MPs.

3.4. Impact of repeated exposure to PE MPs on the human gut microbiota activity in M-ARCOL

3.4.1. Gas and SCFA production

The mean total gas and SCFAs daily produced were first studied as indicators of fermentation activities (Fig. 5a, b). Although exposure to PE MPs had no significant impact on these two parameters, the average daily total gas production (Fig. 5a) tended to decrease in adult 2 and

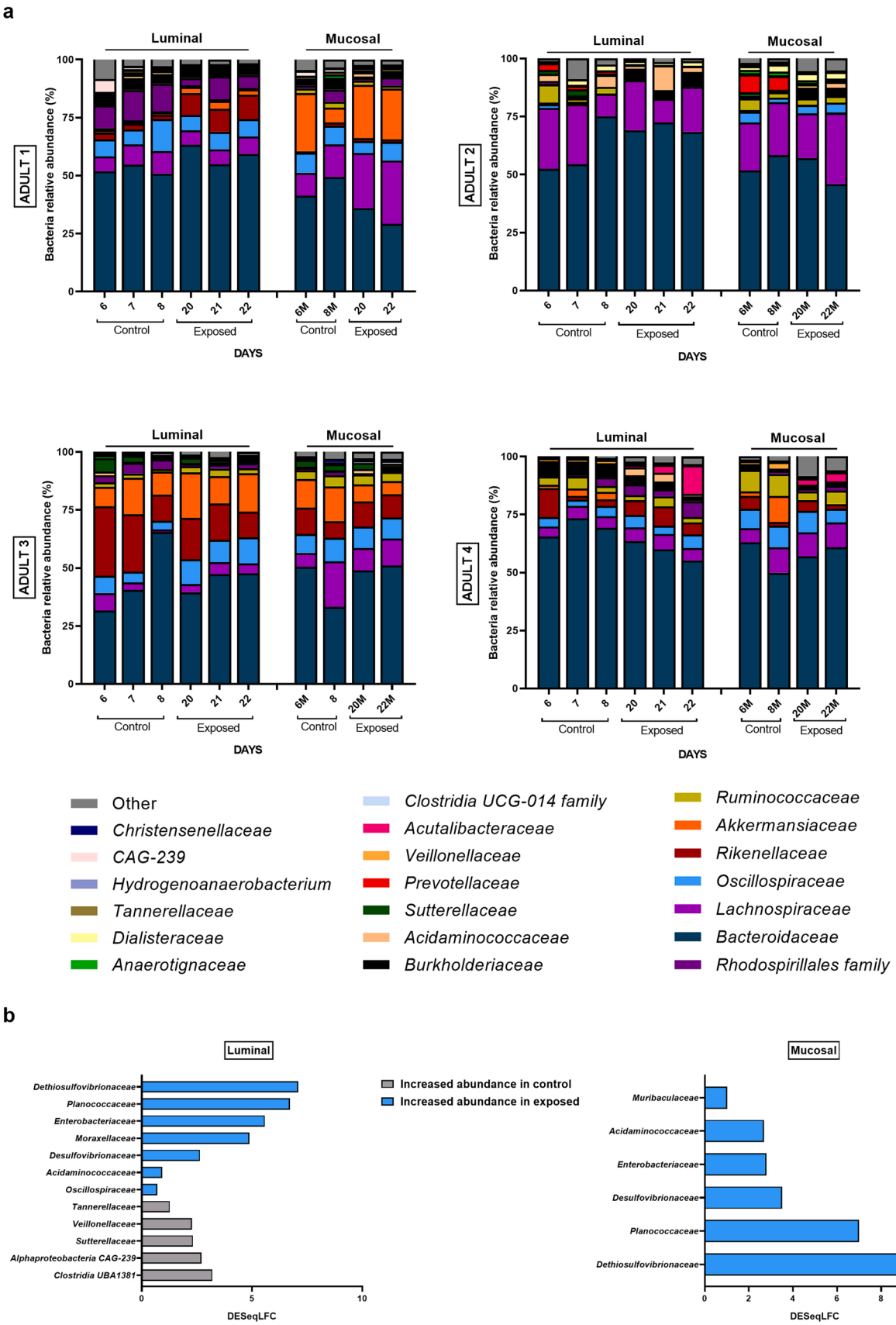

Fig. 2. Effect of repeated exposure to PE MPs in M-ARCOL on luminal and mucosal bacterial microbiota composition at the family level. Bacterial composition was determined by 16S rDNA gene metabarcoding. a) Relative abundance of the 20 main bacterial populations at the family level during the control and exposed periods for each donor. M represents the medium surrounding the mucin-alginate beads. b) Differential Analysis (DESeq2, metagenomeSeq, metacoder, $p < 0.05$) at the family level between control and exposed days (n = 4).

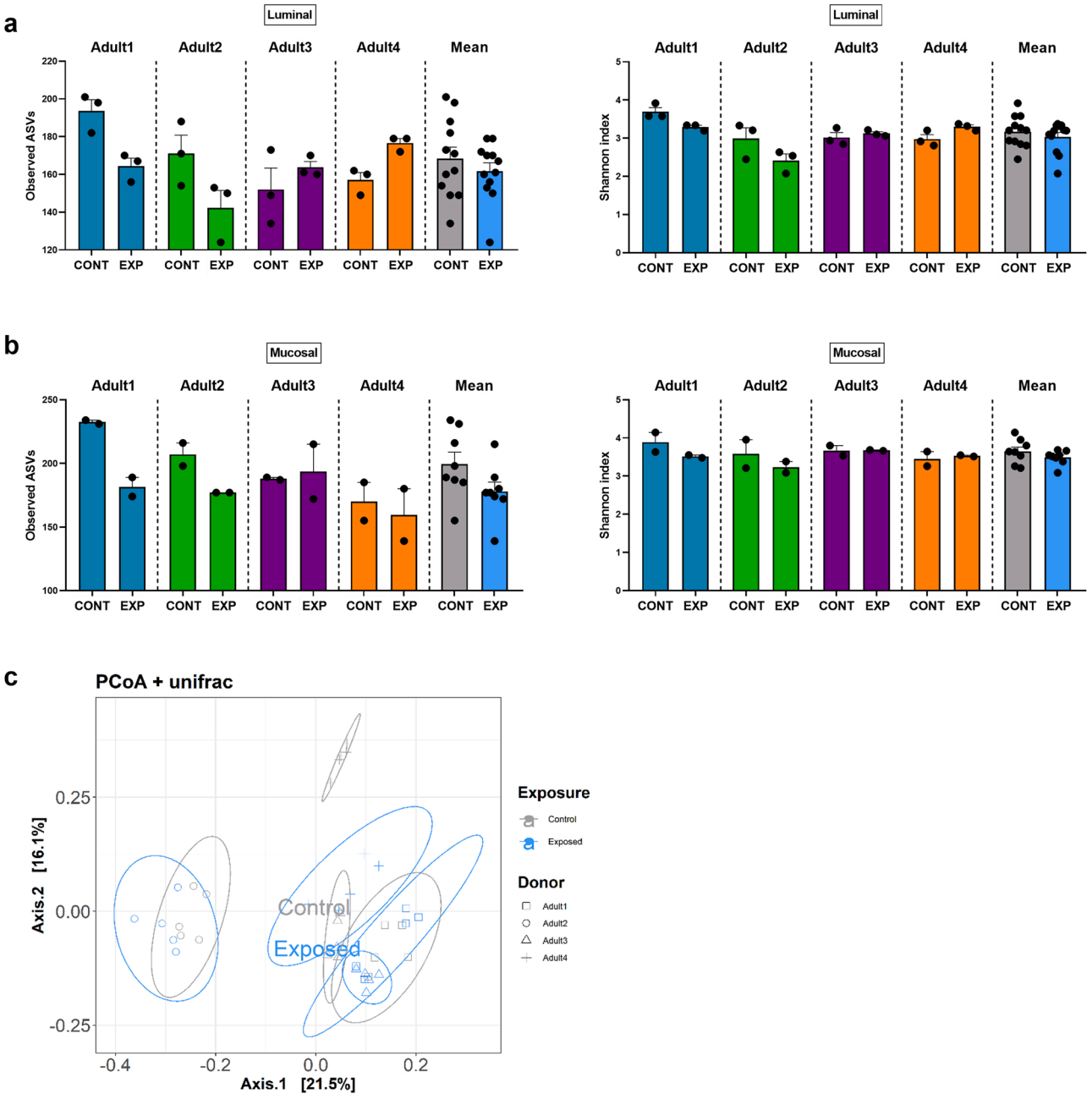

Fig. 3. Effect of repeated exposure to PE MPs in M-ARCOL on α-and β-diversity indexes of bacterial communities. Bacterial composition was determined by 16S rDNA gene metabarcoding. Bacterial α-diversity was calculated and expressed as the number of observed ASVs (a) and as the Shannon index (b) for each donor and as a mean (n = 4) (mean ± SEM). Bacterial β-diversity was also represented (c) using a two-dimensional PCoA plot, based on the unweighted UniFrac distance matrix, on luminal and mucosal samples. *ASVs: amplicon sequence variants; CONT: control, EXP: exposed.*

increase in adult 4 after exposure while the average daily total SCFA production (Fig. 5b) tended to decrease for adult 4. Only adult 2 produced significantly less acetate after exposure to PE MPs (56.9 ± 0.2 vs 54.2 ± 0.1 mM, Brown-Forsythe ANOVA, $p = 0.04$) while acetate production only tended to decrease in adult 4 and to increase in adults 1 and 3. For propionate, adult 3 tended to produce less propionate daily after exposure to PE MPs, as did adult 4. For adult 2, propionate production tended to increase after exposure. Mean daily butyrate production was not significantly impacted by exposure to PE MPs although it was significantly decreased for adult 4 (26.5 ± 0.8 vs 17.1 ± 0.3 mM, one-way ANOVA, $p = 0.03$). The kinetics of total daily gas and SCFA production were also followed (Fig.S6a, b). The profiles of relative gas and SCFA composition (Fig.S6c) were stable for the control period with the exception of the gas profile of adult 2, beginning to produce H_2 at day 5 and up to 25 % for all the remaining days. Of note, adult 3 produced a peak of H_2 (14 %) on day 9, the day after the first injection of PE MPs. Interestingly, adult 4 began to produce CH_4 on day 13. In an attempt to integrate the different datasets, an RDA of the bacterial β-diversity was implemented, based on 16S rDNA gene metabarcoding and metabolic data from the luminal phase only and excluding the strong donor-effect potentially masking the influence of other factors (Fig. 5d). A clear distinction between control and exposed days was observed and several variables explained the difference between the four gut microbiota: total gas and SCFA production, propionate and acetate production. However, the main factor explaining those differences was the exposure to PE MPs.

3.4.2. *Volatolome*

Another robust indicator, although little studied to date in the

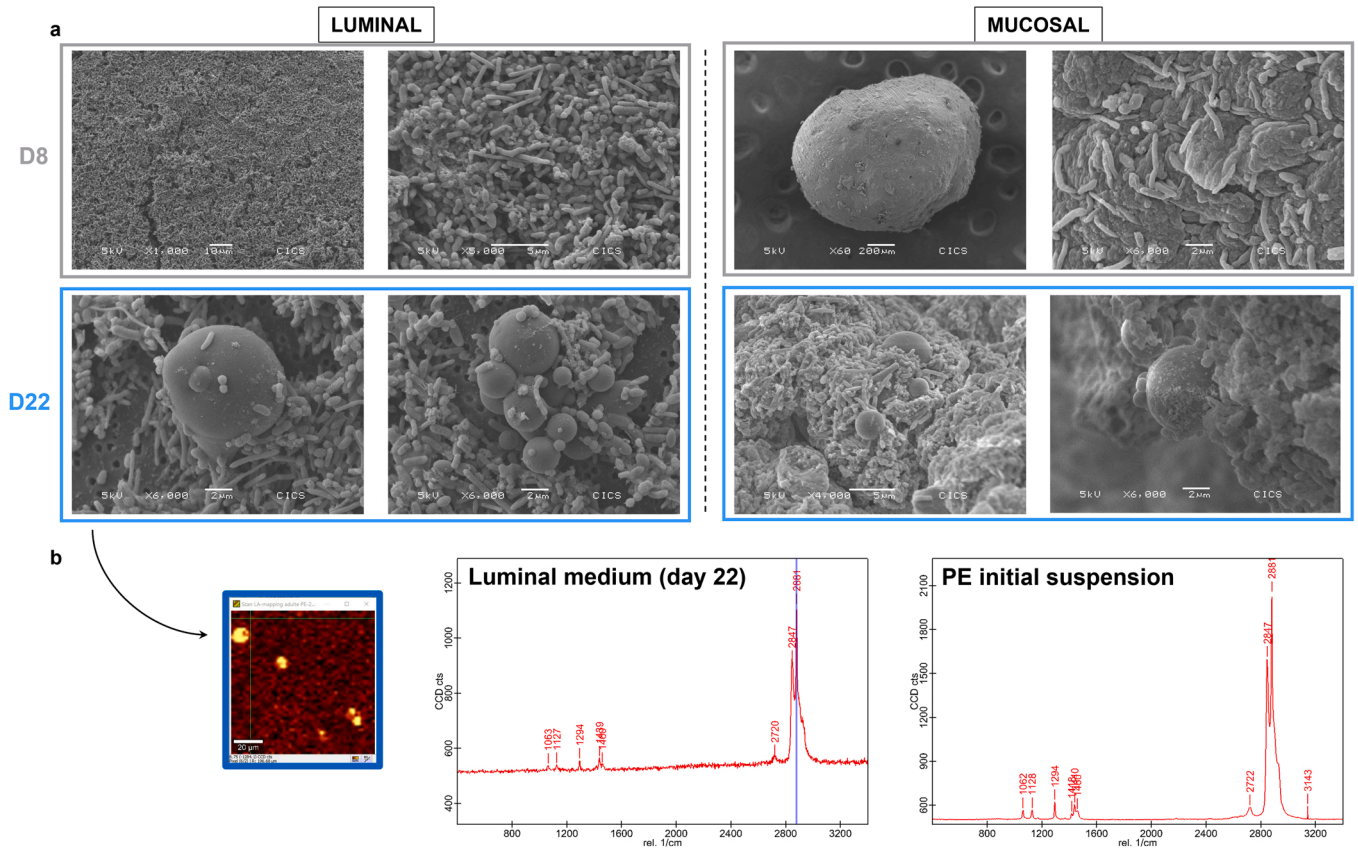

Fig. 4. Scanning electron microscopy observations of PE MPs/gut microbiota interactions in M-ARCOL and Raman spectroscopy analysis of PE MPs at the end of exposed period. (a) Representative scanning electron microscopy images of luminal samples and mucin-alginate beads for adult 3 before (upper panels) and after (lower panels) exposure to MPs. The analysis was performed on mucin-alginate beads after 48 h of colonization in the mucosal external compartment. The right panel at day 8 shows a typical mucin-alginate bead and its colonization by gut microbiota. (b) Representative Raman spectroscopy for adult 3 of PE MPs (map on the left, PE MPs are coloured in yellow; Raman spectra on the right) in the luminal sample at day 22 compared to the initial suspension of PE MPs. *PE: polyethylene.*

literature, of gut microbiota activity is its volatolome. VOCs were identified and quantified for day 8 as 'control' and day 22 as 'exposed' from the luminal samples of the four donors. While a total of 183 VOCs were detected, five had significantly differential abundance between control and exposed samples ($n = 4$, $p < 0.05$) (Table 1). The PCA using the five discriminant VOCs clearly showed the presence of two clusters, corresponding to the control and exposed groups (Fig. 6). Thus, exposure to PE MPs induced specific changes in the volatolomic profile of the gut microbiota. The abundance of these five discriminant VOCs, including three hydrocarbons (pentane, 3-methyl-; cyclopentane, 1,1,3-trimethyl-; 1-heptene, 2,4-dimethyl-), one alcohol (3-nonyn-2-ol) and N-heterocycle compound (indole, 3-methyl-), is shown in Table 1. While the abundance of the three hydrocarbon and alcohol compounds was significantly reduced after exposure to PE MPs, the abundance of indole, 3-methyl- was significantly increased (35-fold increase).

3.4.3. *Activation of AhR*

Finally, we investigated the ability of M-ARCOL luminal supernatants to activate AhR after exposure to PE MPs (day 22) compared with control conditions (day 8) using a reporter cell line. AhR activity was not significantly different after exposure from that obtained with controls (Fig. 7). However, AhR activity tended to be lower for all adults, except for adult 2 for which it was significantly higher (one-way ANOVA, $p < 0.001$), suggesting a potential defect in the microbiota to produce metabolites known to activate this receptor involved in regulation of intestinal homeostasis.

3.5. *Impact of M-ARCOL luminal supernatants on intestinal barrier integrity using a Caco-2/HT29-MTX cell model*

We then investigated the potential impact of M-ARCOL luminal supernatants after exposure to PE MPs (day 22) compared with control conditions (day 8) on the intestinal barrier integrity using co-cultures of Caco-2 and mucus-secreting HT29-MTX cells grown in inserts. The toxicity assay with 1/2, 1/5, 1/10, 1/20 and 1/50 (v/v) dilutions of M-ARCOL luminal supernatants showed no cytotoxicity for 1/20 and 1/50 dilutions (data not shown). Therefore, in the following experiments on Caco-2/HT29-MTX cells, 1/20 (v/v) diluted supernatants were used.

The intestinal barrier function was first assessed by TEER and LY transport measurements. A decrease in TEER values, associated with an increase in LY translocation, is indicative of an increase in intestinal permeability and thus an impairment of intestinal barrier function (Geirnaert et al., 2017). Here, TEER was monitored in situ and in real time with the cellZScope2 system. The difference between the mean TEER values before and after the 24-h incubation period was calculated for all conditions and termed ΔTEER. This parameter was not significantly differentially impacted by the supernatants of the exposed microbiota compared with the control, although it tended to be lower for adults 2 and 3 and higher for adult 4 (Fig. 8a). Consistently, the LY P_{app} was not statistically different between the supernatants from exposed and control gut microbiota, but tended to be higher for adults 1 and 2 and lower for adult 3 (Fig. 8a). Transcellular permeability was also assessed by measuring HRP apparent permeability measurement. Similarly, no significant difference was observed between supernatants from exposed and control gut microbiota, although, as with LY P_{app}, HRP P_{app} tended to be higher for adults 1 and 2 and lower for adults 3 and 4

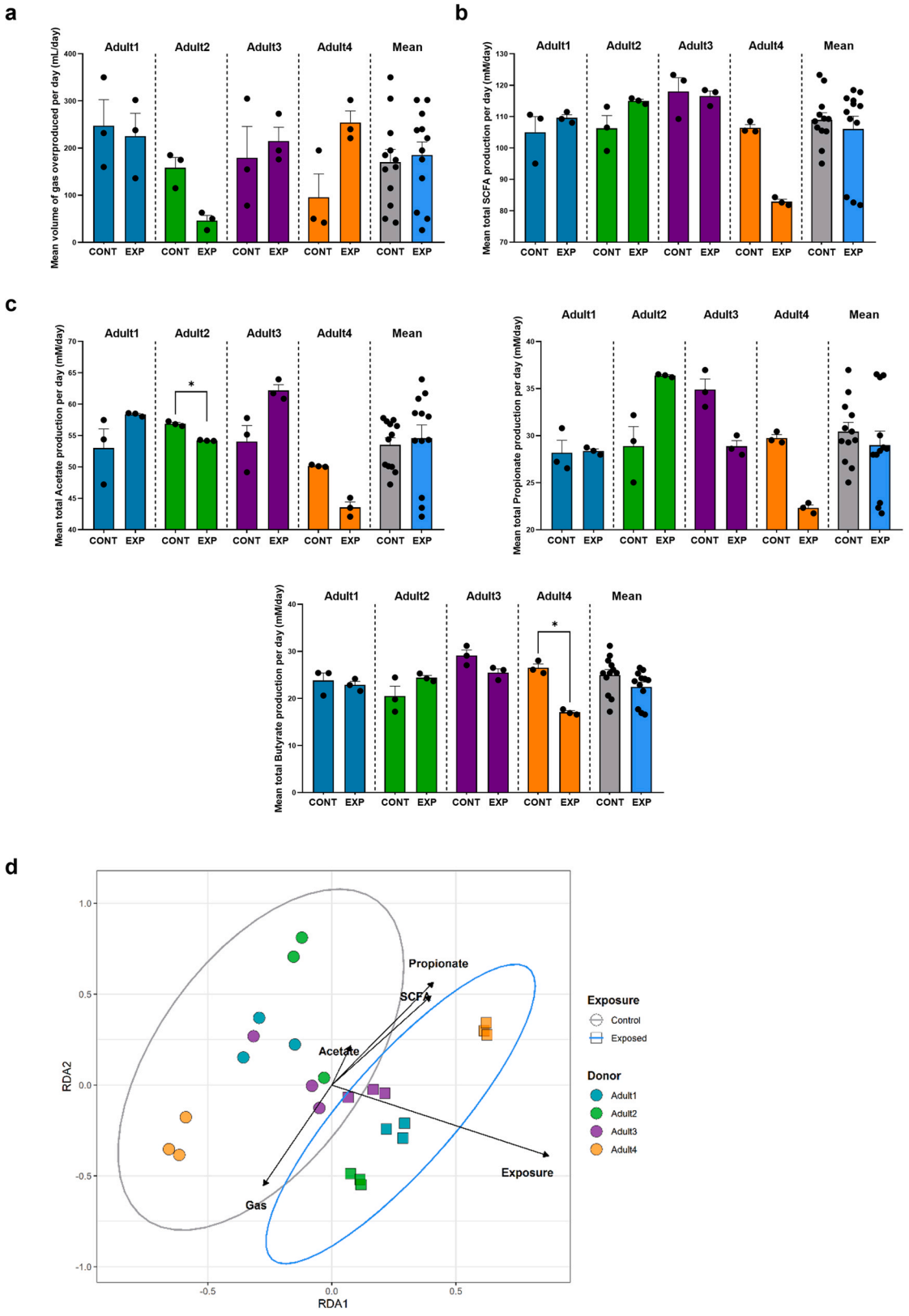

Fig. 5. Impact of repeated exposure to PE MPs on gas and short chain fatty acid production in M-ARCOL. (a) Daily gas production (mean ± SEM in mL) and (b) Total SCFA production (mean ± SEM in mM) for each donor and on average (n = 4). (c) Daily production of acetate, propionate and butyrate (mean ± SEM in mM) for each donor and on average (n = 4). Statistical differences were assessed by one-way ANOVA with $p < 0.05$ for significance. (d) Distance-based redundancy analysis (RDA) based on 16S rDNA gene metabarcoding and metabolic data (gas and SCFAs) applied to luminal samples and excluding the donor effect. *CONT: control; EXP: exposed; SCFAs: short chain fatty acids.*

Table 1
Volatile organic compounds in the volatolome of the fecal microbiota as significantly altered by the repeated exposure to PE MPs.

Candidate markers	Tentatively identification[a]	*m/z*[b]	Exp. RI[c]	Ref. RI[d]	CAS number	*p* value	Control (day 8)	Exposed (day 22)	Under/over production compared to the control
Hydrocarbons									
pentane, 3-methyl-	MS+RI	71	561	578	96–14–0	* **	1.6 (18 %)	0.32 (48 %)	↘
cyclopentane, 1,1,3-trimethyl-	MS	97	728		4516–69–2	* **	1.5 (13 %)	0.38 (40 %)	↘
1-heptene, 2,4-dimethyl-	MS+RI	70	841	855	19549–87–2	*	16 (19 %)	7 (53 %)	↘
Alcohols									
3-nonyn-2-ol	MS	43	1110	NA	26547–25–1	*	11 (36 %)	4.2 (46 %)	↘
N-heterocycle compounds									
indole, 3-methyl-	MS+RI	58	1197	1192	693–54–9	*	12 (149 %)	418 (73 %)	↗

Values are the mean of abundances ($\times 10^5$) of each candidate marker with its standard deviation (in brackets).
[a]MS + RI, mass spectrum and RI agree with literature data; MS, mass spectrum agrees with literature spectrum; [b]Mass fragment used for area determination; [c,d]Retention indices (RI) on a DB5 capillary column from experimental run (c) or bibliographic data (d); NA: Non-available; ↘: under production compared to the control; ↗: over production compared to the control; *p < 0.05; * *p < 0.01; * **p < 0.001 Bonferroni corrected value.

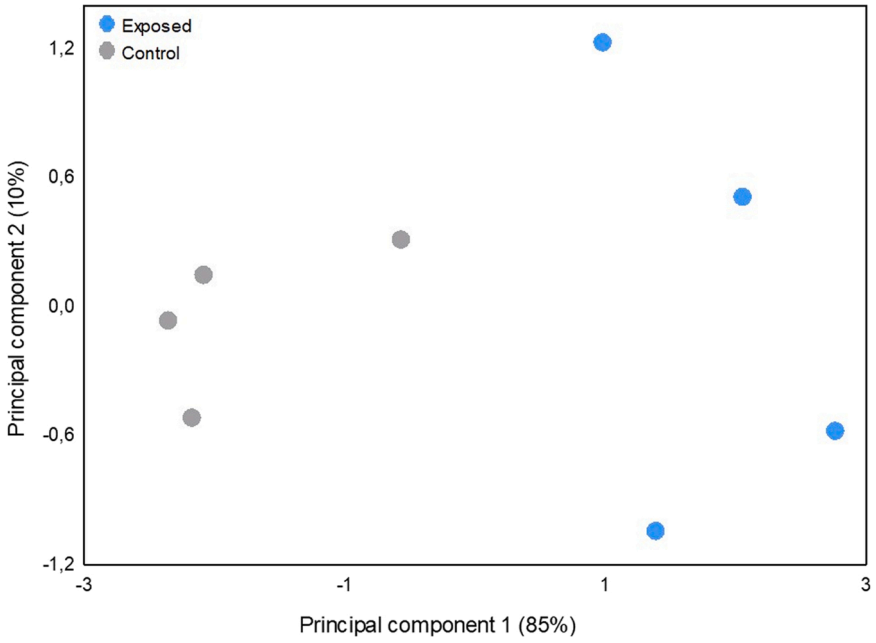

Fig. 6. Impact of repeated exposure to PE MPs in M-ARCOL on volatile organic compounds produced by the gut microbiota in the luminal compartment. Volatile organic compounds (VOCs) were analysed for each adult donor (n = 4) at day 8 and day 22. Principal component analysis (PCA) of the control and exposed days including the five discriminant VOCs described in Table 1.

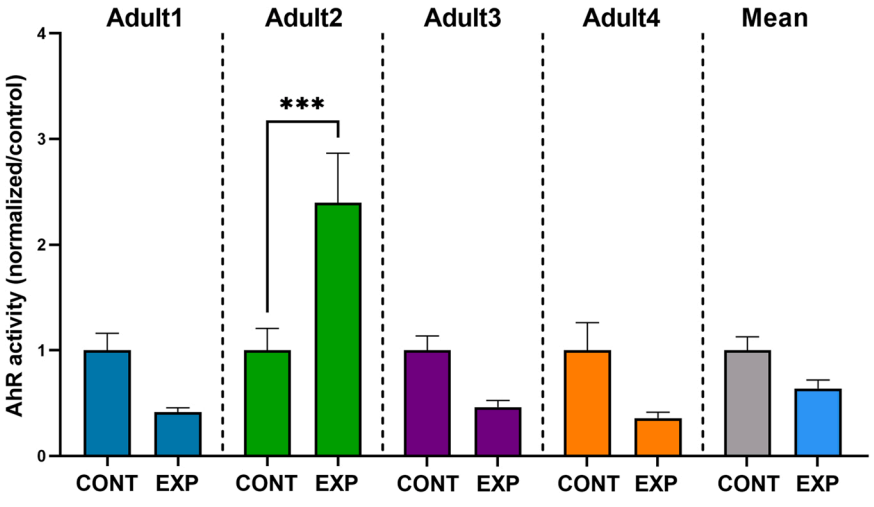

Fig. 7. Ability of luminal M-ARCOL luminal supernatants to activate AhR after exposure to PE MPs. AhR activity is expressed as fold changes relative to the luciferase activity of the control and after normalisation based on sample cytotoxicity using the lactate dehydrogenase activity assay. All results are given for each individual donor and the mean is calculated (mean ± SEM, n = 4). Statistical differences were assessed by one-way ANOVA with $p < 0.05$ for significance. *AhR: aryl hydrocarbon receptor; CONT: control; EXP: exposed.*

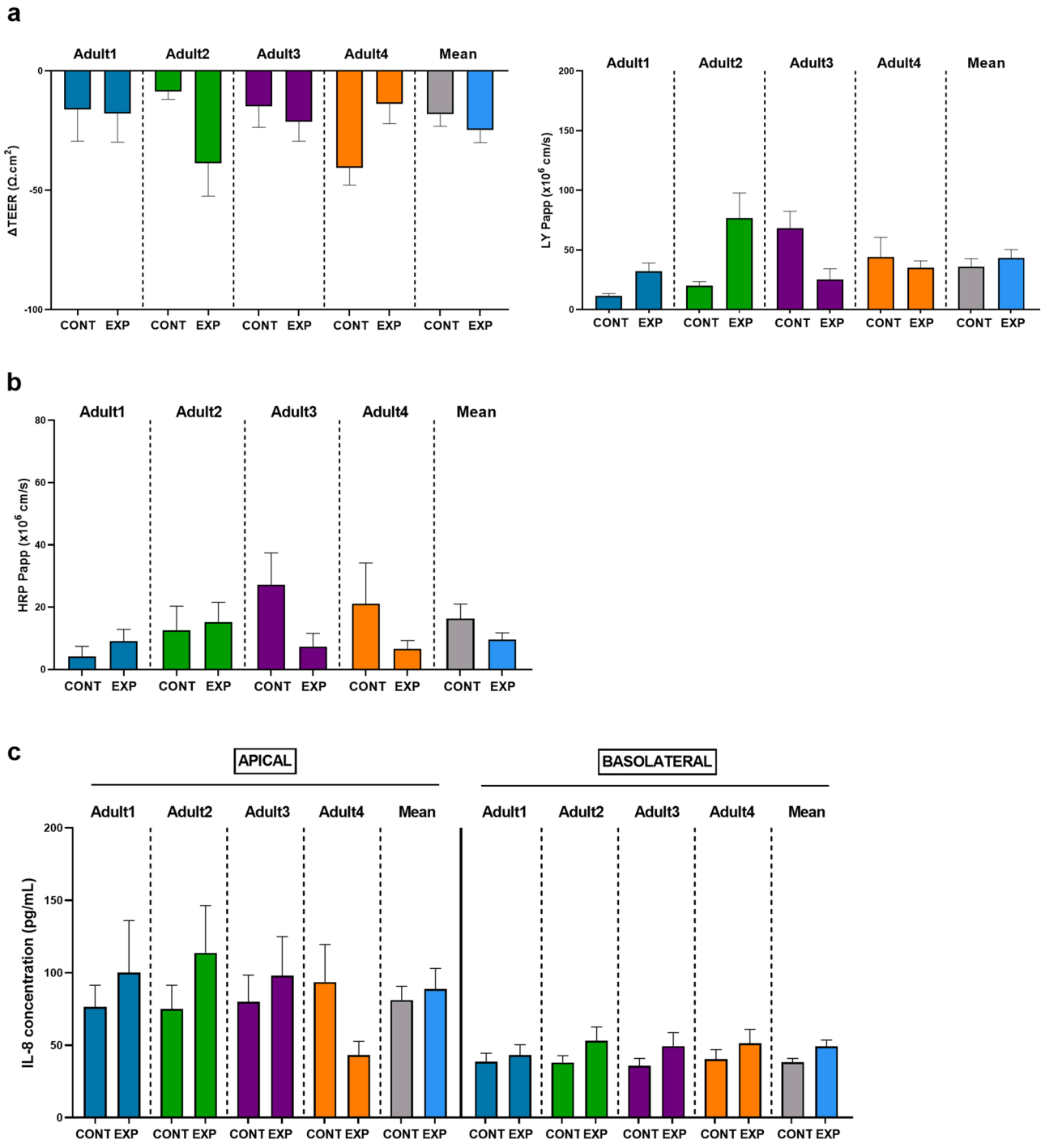

Fig. 8. Impact of luminal supernatants of M-ARCOL before and after repeated exposure to PE MPs on intestinal barrier integrity using a Caco-2/HT29-MTX co-culture. (a) ΔTEER (difference in $\Omega.cm^2$ between mean TEER after and before the 24-h incubation period) and LY transport (Papp in cm/s) as an indicator of intestinal paracellular permeability. (b) HRP transport (Papp in cm/s) as an indicator of intestinal transcellular permeability. (c) Mean IL-8 concentration (in pg/mL) in the apical and basolateral media of the co-culture. All results are given by donors and on average (n = 4) and expressed as means ± SEM. *CONT: control; EXP: exposed; HRP: horseradish peroxidase; IL-8: interleukin-8; LY: lucifer yellow; Papp: apparent permeability coefficient; TEER: trans-epithelial electrical resistance.*

(Fig. 8b). Fully consistent with these permeability measurements, gene expression of *ZO-1* and *OCLN* was not statistically different between the supernatants from exposed and control gut microbiota (Fig.S7a). Of note, unlike *OCLN*, *ZO-1* gene expression tended to decrease in adults 1, 2 and 3 for the exposed gut microbiota supernatant compared with the control. Regarding mucin synthesis, no significant differences in *MUC2* and *MUC5AC* gene expression were observed (Fig.S7b). Interestingly, *MUC5AC* gene expression tended to increase in adults 1 and 3 for the exposed gut microbiota supernatant compared with the control.

Finally, no significant difference in apical production of the pro-inflammatory cytokine IL-8 was reported between the supernatants of exposed and control gut microbiota, but it tended to be higher for all adults except adult 4 (Fig. 8c). In the basolateral compartment, IL-8 production, generally lower than in the apical compartment, tended to be increased for the exposed gut microbiota supernatant compared with the control for all donors.

4. Discussion

Given the converging and critical evidence of human exposure to MPs, our study is the first to assess in adults the impact of PE MPs on the human digestive ecosystem in vitro under realistic conditions, i.e. repeated exposure for 14 days at a dose (21 mg/day) in agreement with exposure data reported so far in the literature for humans (from 14 to 714 mg per day) (Senathirajah et al., 2021). To this endeavor, we simulated the human adult digestive environment by coupling the M-ARCOL colonic model with a co-culture of human intestinal cells mimicking the mucus/epithelium axis.

The gut microbiota has been identified as a key player in the host toxicity of xenobiotics (Claus et al., 2016). While the gut microbiota has a high capacity to metabolize various environmental chemicals, xenobiotics also alter the composition and/or metabolic activity of gut microbial communities (Lindell et al., 2022). Our study focused on elucidating the interplay between the gut microbiota and PE MPs. It should be noted that the initial fecal microbiota used for M-ARCOL inoculation showed strong inter-individual variabilities, which were maintained in vitro throughout the experiment, as evidenced by adults 3 and 4. However, both were profoundly affected by exposure to PE MPs as clear changes in β-diversity were observed after treatment, accompanied by a trend of increasing α-diversity (observed ASVs) for the luminal microbiota. Despite the inter-individual variability, specific effects were associated with the lumen and mucus-associated microbiota. While an increase in well-known gut pathobionts *Dethiosulfovibrionaceae*, *Enterobacteriaceae*, *Desulfovibrionaceae* (Liu et al., 2020b; Zhang et al., 2021c; Pittayanon et al., 2019) was observed after exposure to PE MPs for both luminal and mucosal microbiota, a decrease in *Christensenellaceae* and *Akkermansiaceae,* two populations associated with a healthy state (Waters and Ley, 2019; Hasani et al., 2021), were observed for two donors in the mucosal compartment. Some of the variations in the structure of the gut microbiota obtained here are close to the microbial specificities described in irritable bowel syndrome and inflammatory diseases of the gastrointestinal tract (Pittayanon et al., 2019; Zhu et al., 2018). To date, only one study has investigated the impact of MPs on the human gut microbiota under physiologically relevant digestive conditions in vitro. Tamargo and her team used a complex in vitro colonic system, SIMGI®, which recreates the different regions of the lower gut (ascending, transverse and descending colon) (Tamargo et al., 2022). A single dose of polyethylene terephthalate (PET) MPs (0.166 g), previously digested by a standardized in vitro static digestion method, was administered for 72 h into the SIMGI® model inoculated in parallel with fecal samples from two donors. The authors observed compartment- and donor-dependent effects. Following exposure to PET MPs, a decrease in *Bacteroidota* (previously named *Bacteroidetes*) was observed in all three colonic compartments for both donors. An increase in *Desulfobacterota* was also reported in all three compartments for one donor but not in the transverse colon for the other. The *Synergistetes* population was increased in the transverse and descending colon for one donor but only in the descending colon for the other. Surprisingly, while *Proteobacteria* were increased in the transverse colon of one donor, they were decreased in the ascending and transverse colon of the second donor. In our experiments, we also observed an increase in *Synergistetes* and *Proteobacteria* at lower taxonomic levels.

Despite major discrepancies between human and mouse digestive conditions and gut microbiota characteristics (Hugenholtz and de Vos, 2018), it is interesting to report effects on gut microbiota composition after exposure to PE MPs in murine models. An increase in the abundance and diversity of the fecal microbiota has been reported after exposure to PE MPs (10–150 μm) (Li et al., 2020), which was associated with a higher abundance of *Staphylococcus*, as well as a reduction in *Parabacteroides* abundance, compared to untreated animals. More recently, variations in the composition of the gut microbiota have been reported in mice orally exposed to PE MPs of two sizes (36 and 116 μm), characterized in particular by less abundant *Verrucomicrobiales* and more abundant *Gastranaerophilales* compared to their unexposed counterparts (Djouina et al., 2022). While the affected populations reported in the above studies were different from those we observed, similar results were found in vivo with other types of MP polymer. Notably, exposure of mice to 2-μm polyvinylchloride (PVC) MPs (Chen et al., 2022) led to a higher level of *Proteobacteria* in the exposed group compared with the control, whereas exposure to polystyrene (PS) MPs (mixture of 5-, 50-, 100- and 200-μm particles) in mice fed a normal or high-fat diet resulted in an increase in the relative abundance of *Enterobacteriaceae* and *Desulfovibrionaceae* (Huang et al., 2022). In addition, another study with 5-μm PS MPs also showed a significant increase in *Proteobacteria* and *Enterobacteriaceae* as well as potentially pro-inflammatory bacteria and pathogens, such as *Desulfovibrio* and *Oscillospiraceae*, which was also observed in our study (Wen et al., 2022). These observations highlight the importance of identifying, in addition to the exposure scenario, the main properties of the MPs involved, e.g. type or size of plastic, as highlighted previously (Stock et al., 2022).

Our study is the first one investigating the potential effect of exposure to PE MPs on the production of gas, VOCs and SCFAs by the human gut microbiota. Interestingly, the effect of PE MPs on these parameters was not so striking, but the trend, as with gut microbiota composition, appeared to be donor-dependent. To date, studies examining microbial VOCs are scarce and only a few databases indexing these microbial VOCs are currently available (Agarwal et al., 2016; Abdullah et al., 2015; Lemfack et al., 2014). However, these compounds play important roles in biological interactions between organisms and are increasingly used as biomarkers for various human diseases, including cancer, gastrointestinal and metabolic disorders (Arasaradnam et al., 2014; Schenkel et al., 2015; Walton et al., 2013; Garner et al., 2007). Exposure to PE MPs significantly altered the microbial volatile profile, characterized by five major discriminant VOCs. While the abundance of three hydrocarbon and one alcohol compounds was decreased after exposure to PE MPs, the abundance of indole, 3-methyl- was drastically increased. This compound, also known as skatole, is a tryptophan-derived metabolite absorbed by the gut epithelium and synthesized by the gut microbiota in the small intestine and the colon from indole-3-acetic acid via a decarboxylation process (Yokoyama and Carlson, 1979). Because its production requires two steps mediated by at least two different bacterial species (*Bacteroides*, *Clostridia* or *Escherichia coli* and *Lactobacillus*, *Clostridium*, *Desulfovibrio* or *Bacteroides*) (Cook et al., 2007; Smith and Macfarlane, 1997), its level is generally low. Interestingly, the *Desulfovibrio* population, which is increased in our study, might be involved in skatole production (Shi et al., 2020) and might explain, at least in part, the increased skatole production. In healthy individuals, skatole was not detected during fermentation in the large intestine (Smith and Macfarlane, 1997), whereas high skatole concentrations were reported in the gut of patients suffering from saccharo-butyric putrefaction (Herter, 1908) and in the serum of patients with hepatic encephalopathy (Suyama and Hirayama, 1988). This drastic increase in indole, 3-methyl- or skatole abundance may indicate potential microbiota-mediated gastrointestinal dysregulation after exposure to PE MPs and thus warrants further investigations.

Finally, we evaluated the ability of the gut microbiota to activate AhR after exposure to PE MPs. Several environmental chemicals have been characterized as triggering an AhR-mediated pro-inflammatory response in different cell types (Henley et al., 2004; Tamaki et al., 2004; Pei et al., 2002). The gut microbiota has the ability to produce tryptophan-based AhR ligands (e.g. tryptamine, indole-3-acrylic acid, indole-3-acetic acid, indole-3-acetaldehyde or indole-3-aldehyde) influencing the intestinal epithelial integrity but also the development, function, production and maintenance of several key mucosal immune cells and mediators (Lamas et al., 2018; Agus et al., 2018; Roager and Licht, 2018; Rothhammer and Quintana, 2019). Of note, skatole was shown to have a moderate agonist effect on human AhR compared with other microbial intestinal tryptophan catabolites (Vyhlídalová et al., 2020). A deficit in AhR ligand production by the gut microbiota has been

reported in inflammatory bowel disease, celiac disease and obese patients compared to healthy subjects (Lamas et al., 2016, 2020; Natividad et al., 2018). In our study, AhR activity tended to be lower with the supernatant of PE-MP exposed gut microbiota compared to the respective control for all donors except adult 2. These results suggest a lower production of tryptophan-based AhR ligands by the gut microbiota after exposure to PE MPs, which could promote intestinal inflammation, as previously observed in celiac disease (Lamas et al., 2020).

We next investigated how the gut microbiota may interact reciprocally with PE MPs. SEM images revealed the presence of microorganisms attached to the surface of PE MPs. The formation of "biofilm-like" microbial communities on the surface of PET MPs was already reported by Tamargo and colleagues (Tamargo et al., 2022), but not on PE MPs. In the environment, depending on the MP surrounding medium, biofilms of various microorganisms can be deposited on the particle surface. These specific communities are called the 'plastisphere' (Zettler et al., 2013). *Alphaproteobacteria*, *Gammaproteobacteria* and *Bacteroidia* were identified as the core microbiome of the PE-associated biofilms in seawater (Tu et al., 2020) and are also phyla encountered in the gut microbiota. In addition, Tang and colleagues recently confirmed the adhesion of *E. coli* (*Enterobacteriaceae* family), a well-known member of the gut microbiota, on the surface of PE MPs (Tang et al., 2022). While Tamargo and co-workers reported a progressive amorphisation of the PET MP surface especially during colonic fermentation in SIMGI®, no major modification of the polymeric composition of PE MPs was demonstrated in our study by Raman spectroscopy, after contact with the gut microbiota. Interestingly, biodegradation of LDPE was reported in enrichment cultures with this polymer as the main carbon source for two environmental species from *Proteobacteria* phylum (*Microbulbifer* sp and *Alcanivorax borkumensis,* the latter being described as an excellent candidate for degradation of petroleum-based plastics such as LDPE), while the *Desulfovibrionaceae* family would include members of the LDPE plastisphere (Delacuvellerie et al., 2019). These results support the hypothesis of interactions between microorganisms and PE MPs in the gut. Thus, the potential degradation of MPs (PE but also other types of polymer) by the human gut microbiota would deserve further research, although the limited contact time in the human gut during gastrointestinal transit does not favor plastic degradation, compared to longer exposure to soil or water microorganisms in the environment (Akarsu et al., 2022; Tareen et al., 2022; Giangeri et al., 2022).

We next evaluated for the first time the impact of M-ARCOL luminal supernatants before and after exposure to PE MPs exposure on the co-culture of Caco-2 and mucus-secreting HT29-MTX human intestinal cells to simulate the gut microbiota/mucus/epithelium axis. No major effects were observed on intestinal para- and trans- permeabilities, mucin synthesis or IL-8 production, probably due to the few changes observed in the profiles of gut microbiota metabolites (e.g. SCFAs or AhR ligands) after exposure. Although no studies to date have evaluated the indirect effects of PE MPs, mediated by changes in microbial metabolites, on the mucus/epithelium barrier, the direct impact of exposure to PE MPs on these parameters has already been studied in vivo. In particular, in mice exposed to PE MPs of two sizes (36 and 116 μm), the authors reported an increase in mucosal and mucin areas and, in particular, an upregulation of *Muc2* transcripts in the colon, reflecting dysregulation of colonic mucosa differentiation (Djouina et al., 2022). Moreover, Sun and colleagues showed for smaller PE MPs (1–10 μm) a decrease in mucin production but not *Muc2* mRNA levels in mice (Sun et al., 2021). A pro-inflammatory state after exposure to PE MPs was also reported in mice with 10–150 μm particles (Li et al., 2020). *In vitro*, the impact on intestinal cells, in monoculture or co-culture, has been evaluated via direct exposure to MPs. For example, exposure of Caco-2 cells to two sizes of PE MPs (30.5 ± 10.5 and 6.2 ± 2.0 μm) did not significantly reduce cell viability except slightly at high concentration (1000 μg/mL) (Gautam et al., 2022) but induced oxidative stress, as illustrated by nitric oxide and reactive oxygen species markers. Interestingly, Hesler and colleagues studied the impact of PS small-sized particles (500 nm) on a co-culture of Caco-2 cells with HT29-MTX-E12 cells, but found no significant cytotoxicity, unless applied at very high concentrations, nor barrier integrity impairment, thus highlighting a possible protective effect of the mucus layer (Hesler et al., 2019).

Despite the substantial progress regarding the impact of MPs on the human digestive environment, our study has some limitations. First, we only considered virgin PE microbeads even though the spherical shape is not fully representative of ingested forms (e.g. fibers or fragments (Fournier et al., 2021a)). Indeed, MPs are complex particles, characterized by many different parameters, including the type of polymer, size, shape, surface properties, presence of adsorbed contaminants (Yu et al., 2019) and/or the formation of a biomolecular corona, for example after human digestion (Stock et al., 2019). Furthermore, while virgin MPs can simulate a direct source of human exposure (e.g. from food packaging), the use of weathered particles is important to simulate environmental exposure as weathering leads to strong physico-chemical changes in MPs (Liu et al., 2019). This highlights the critical need to disentangle the effects of "real-life" MPs, which are likely to exhibit distinct physico-chemistry, behavior and toxicity towards the human digestive environment.

In addition, we only studied healthy adult volunteers here. However, assessing the toxicological consequences on at-risk populations such as infants, in fit-for-purpose in vitro gut models (Fournier et al., 2021b), would be highly relevant since it has been recently shown that MPs are more abundant in the stools of infants than in adults (Zhang et al., 2021a). Similarly, pathophysiological conditions (e.g. patients with inflammatory bowel disease (IBD)) could be simulated in the M-ARCOL gut model. Indeed, in these "sensitized" individuals with defective mucus/epithelial barriers and dysbiotic gut microbiota (Stange and Schroeder, 2019), the fecal concentration of MPs was significantly higher than that in their healthy counterparts (Yan et al., 2022). Interestingly, a positive correlation was found between the fecal concentration of MPs and the IBD severity (Yan et al., 2022), although the underlying mechanisms remain far from understood.

5. Conclusions

Our study investigated for the first time the impact of a 2-week repeated exposure to PE MPs at a relevant dose on the human digestive ecosystem in adults, by coupling the in vitro colonic model M-ARCOL with a co-culture of Caco-2/HT29-MTX intestinal cells to simulate the gut microbiota/mucus/epithelium axis. Taken together, our results showed effects of PE MPs on the luminal and mucosal gut microbiota, both in terms of composition and metabolic activity, to a different degree and in an individual-dependent manner. Such exposure may promote the development of human pathobionts (e.g. *Desulfovibrionaceae* and *Enterobacteriaceae,* as seen both for the luminal and mucosal compartments) at the expense of beneficial bacteria (e.g. *Christensenellaceae* and *Akkermansiaceae* in the mucosal microbiota). The production of gas and metabolites (i.e. SCFAs and tryptophan-based AhR ligands) by the human gut microbiota after exposure to PE MPs was not significantly affected although the microbial volatolome was altered with, in particular, an increased production of indole, 3-methyl- (or skatole). We also focused on the interactions of microorganisms from the gut microbiota with PE MPs without biodegradation at the fermentation time scale used in our experiments, probably due to the chemical stability of this type of polymer. Furthermore, no significant impact of exposure to PE MPs, as mediated by changes in gut microbial metabolites, was reported on the mucus/epithelium barrier in terms of permeability and inflammation. Further studies are now needed to characterize the specific "gut plastisphere" in terms of composition but also metabolism. Other developments can be envisaged for the M-ARCOL/cell culture combination, such as the use of more representative MPs (morphology, surface properties (weathering)), including a digestion step, which can influence physico-chemical properties of MPs (e.g. formation of biomolecular corona). The consequences of MP exposure

on at-risk populations like infants, as well as in pathophysiological conditions (e.g. inflammatory bowel disease patients), could also be determined for a better human health risk assessment.

Funding

This work was supported by a grant from the French Ministère de l'Enseignement Supérieur et de la Recherche to EF and UMR MEDIS, by the National Research Institute for Agriculture, Food and Environment (INRAE, France, PlasToX project) and by the French National Research Agency (ANR-19-MRS2–0011 HuPlastiX project) to MMB.

CRediT authorship contribution statement

Elora Fournier: Conceptualization; Data curation; Formal analysis; Methodology; Funding acquisition; Investigation; Supervision; Writing - original draft. **Mathilde Leveque:** Data curation; Formal analysis; Investigation; Methodology; Validation. **Philippe Ruiz:** Methodology; Validation. **Jeremy Ratel:** Formal analysis; Investigation; Validation; Writing - review & editing **Claude Durif:** Investigation **Sandrine Chalancon:** Investigation **Frederic Amiard:** Formal analysis; Methodology; Validation; Writing - review & editing **Mathieu Edely:** Formal analysis; Methodology **Valerie Bezirard:** Methodology **Eric Gaultier:** Methodology; Validation **Bruno Lamas:** Methodology; Validation; Writing - review & editing **Eric Houdeau:** Resources **Fabienne Lagarde:** Methodology; Validation; Writing - review & editing **Erwan Engel:** Formal analysis; Validation; Writing - review & editing **Lucie Etienne-Mesmin:** Conceptualization; Funding acquisition; Project administration; Supervision; Validation; Writing - review & editing **Stéphanie Blanquet-Diot:** Conceptualization; Funding acquisition; Project administration; Supervision; Validation; Writing - review & editing **Muriel Mercier-Bonin:** Conceptualization; Funding acquisition; Project administration; Supervision; Validation; Writing - review & editing.

Declaration of Competing Interest

The authors declare that they have no known competing financial interests or personal relationships that could have appeared to influence the work reported in this paper.

Data availability

Data will be made available on request.

Acknowledgements

The authors thank Etienne Rifa from the GeT-Biopuces platform (INSA/TBI, Toulouse, France) for help with bioinformatics analysis. The authors are grateful to Frederic Mercier and Nathalie Kondjoyan (MASS Team, INRAE UR370 QuaPA, France) for their involvement in the volatolomic analyses. The authors thank Christelle Blavignac, Centre Imagerie Cellulaire Santé (CICS, UCA PARTNER, France), for her technical support and expertise in SEM analysis. The authors thank Régis Vaudemont (Luxembourg Institute of Science and Technology (LIST), Luxembourg) for his involvement in DSC and TGA measurements and Thierry Falher, Arnaud Littner and Gilles Dennler (French Technical Industrial Centre of the plastics and composites, Bellignat, France) for helpful discussion regarding physico-chemical characterization of PE MPs.

Financial interests

The authors declare that the research was conducted in the absence of any commercial or financial relationships that could be considered as a potential conflict of interest.

Data availability

Raw data are available at NCBI under the Sequence Read Archive database in the BioProject n°PRJNA831017.

Ethics approval

This study is a non-interventional study with no additions to usual clinical cares. The protocol does not require approval from an ethics committee according to the French Public Health Law (CSP Art L 1121–1.1).

Environmental implication

The last half-century has sustained a bloom in plastic production leading to environmental pollution, with formation of microplastics (MPs). Their omnipresence along the food chain has raised concern for human health. While the gastro-intestinal tract is the first exposed surface, the impact of MPs in the human digestive sphere is largely unknown. We investigated the effects of a repeated oral exposure to polyethylene MPs using an original in vitro approach. This work provides a better understanding of interactions between MPs, gut microbiota and mucus, considering inter-individualities, and increases our knowledge on the health hazards of exposure to environmental MP pollution.

Appendix A. Supporting information

Supplementary data associated with this article can be found in the online version at doi:10.1016/j.jhazmat.2022.130010.

References

Abdullah, A.A., Altaf-Ul-Amin, M., Ono, N., Sato, T., Sugiura, T., Morita, A.H., Katsuragi, T., Muto, A., Nishioka, T., Kanaya, S., 2015. Development and mining of a volatile organic compound database. Biomed. Res. Int. 2015, 139254 https://doi.org/10.1155/2015/139254.

Agarwal, S.M., Sharma, M., Fatima, S., 2016. VOCC: a database of volatile organic compounds in cancer. RSC Adv. 6, 114783–114789. https://doi.org/10.1039/C6RA24414A.

Agus, A., Planchais, J., Sokol, H., 2018. Gut microbiota regulation of tryptophan metabolism in health and disease. Cell Host Microbe 23, 716–724. https://doi.org/10.1016/j.chom.2018.05.003.

Akarsu, C., Özdemir, S., Ozay, Y., Acer, Ö., Dizge, N., 2022. Investigation of two different size microplastic degradation ability of thermophilic bacteria using polyethylene polymers. Environ. Technol. 1–22. https://doi.org/10.1080/09593330.2022.2071638.

Altschul, S.F., Gish, W., Miller, W., Myers, E.W., Lipman, D.J., 1990. Basic local alignment search tool. J. Mol. Biol. 215, 403–410. https://doi.org/10.1016/S0022-2836(05)80360-2.

Andoh, A., 2016. Physiological role of gut microbiota for maintaining human health. Digestion 93, 176–181. https://doi.org/10.1159/000444066.

AnonPlasticsEurope, The Facts 2021 - An analysis of European plastics production, demand and waste data, (2021). <⟨www.plasticseurope.org/application/files/9715/7129/9584/FINAL_web_version_Plastics_the_facts2019_14102019.pdf⟩>.

Arasaradnam, R.P., Covington, J.A., Harmston, C., Nwokolo, C.U., 2014. Review article: next generation diagnostic modalities in gastroenterology–gas phase volatile compound biomarker detection. Aliment Pharm. Ther. 39, 780–789. https://doi.org/10.1111/apt.12657.

Birchenough, G.M.H., Johansson, M.E.V., 2020. Forming a mucus barrier along the colon. Science 370, 402–403. https://doi.org/10.1126/science.abe7194.

Bucci, K., Tulio, M., Rochman, C.M., 2019. What is known and unknown about the effects of plastic pollution: a meta-analysis and systematic review. Ecol. Appl. https://doi.org/10.1002/eap.2044.

Callahan, B.J., McMurdie, P.J., Rosen, M.J., Han, A.W., Johnson, A.J.A., Holmes, S.P., 2016. DADA2: High-resolution sample inference from Illumina amplicon data. Nat. Methods 13, 581–583. https://doi.org/10.1038/nmeth.3869.

Capone, S.H., Dufresne, M., Rechel, M., Fleury, M.-J., Salsac, A.-V., Paullier, P., Daujat-Chavanieu, M., Legallais, C., 2013. Impact of alginate composition: from bead mechanical properties to encapsulated HepG2/C3A cell activities for in vivo implantation. PLoS One 8, e62032. https://doi.org/10.1371/journal.pone.0062032.

Chen, X., Zhuang, J., Chen, Q., Xu, L., Yue, X., Qiao, D., 2022. Chronic exposure to polyvinyl chloride microplastics induces liver injury and gut microbiota dysbiosis based on the integration of liver transcriptome profiles and full-length 16S rRNA sequencing data. Sci. Total Environ., 155984 https://doi.org/10.1016/j.scitotenv.2022.155984.

Claus, S.P., Guillou, H., Ellero-Simatos, S., 2016. The gut microbiota: a major player in the toxicity of environmental pollutants. Npj Biofilms Micro 2, 16003. https://doi.org/10.1038/npjbiofilms.2016.3.

Cook, K.L., Rothrock Jr, M.J., Loughrin, J.H., Doerner, K.C., 2007. Characterization of skatole-producing microbial populations in enriched swine lagoon slurry. FEMS Microbiol. Ecol. 60, 329–340. https://doi.org/10.1111/j.1574-6941.2007.00299.x.

Defois, C., Ratel, J., Denis, S., Batut, B., Beugnot, R., Peyretaillade, E., Engel, E., Peyret, P., 2017. Environmental pollutant benzo[a]pyrene impacts the volatile metabolome and transcriptome of the human gut microbiota. Front Microbiol 8, 1562. https://doi.org/10.3389/fmicb.2017.01562.

Defois, C., Ratel, J., Garrait, G., Denis, S., Le Goff, O., Talvas, J., Mosoni, P., Engel, E., Peyret, P., 2018. Food chemicals disrupt human gut microbiota activity and impact intestinal homeostasis as revealed by in vitro systems. Sci. Rep. 8, 11006. https://doi.org/10.1038/s41598-018-29376-9.

Delacuvellerie, A., Cyriaque, V., Gobert, S., Benali, S., Wattiez, R., 2019. The plastisphere in marine ecosystem hosts potential specific microbial degraders including Alcanivorax borkumensis as a key player for the low-density polyethylene degradation. J. Hazard. Mater. 380, 120899 https://doi.org/10.1016/j.jhazmat.2019.120899.

Deschamps, C., Fournier, E., Uriot, O., Lajoie, F., Verdier, C., Comtet-Marre, S., Thomas, M., Kapel, N., Cherbuy, C., Alric, M., Almeida, M., Etienne-Mesmin, L., Blanquet-Diot, S., 2020. Comparative methods for fecal sample storage to preserve gut microbial structure and function in an in vitro model of the human colon. Appl. Microbiol Biotechnol. https://doi.org/10.1007/s00253-020-10959-4.

Djouina, M., Vignal, C., Dehaut, A., Caboche, S., Hirt, N., Waxin, C., Himber, C., Beury, D., Hot, D., Dubuquoy, L., Launay, D., Duflos, G., Body-Malapel, M., 2022. Oral exposure to polyethylene microplastics alters gut morphology, immune response, and microbiota composition in mice. Environ. Res, 113230. https://doi.org/10.1016/j.envres.2022.113230.

Erni-Cassola, G., Zadjelovic, V., Gibson, M.I., Christie-Oleza, J.A., 2019. Distribution of plastic polymer types in the marine environment; a meta-analysis. J. Hazard Mater. 369, 691–698. https://doi.org/10.1016/j.jhazmat.2019.02.067.

Etienne-Mesmin, L., Chassaing, B., Desvaux, M., De Paepe, K., Gresse, R., Sauvaitre, T., Forano, E., de Wiele, T.V., Schüller, S., Juge, N., Blanquet-Diot, S., 2019. Experimental models to study intestinal microbes-mucus interactions in health and disease. FEMS Microbiol. Rev. 43, 457–489. https://doi.org/10.1093/femsre/fuz013.

Fournier, E., Etienne-Mesmin, L., Blanquet-Diot, S., Mercier-Bonin, M., 2020. Impact of microplastics in human health. In: Rocha-Santos, T., Costa, M., Mouneyrac, C. (Eds.), Handbook of Microplastics in the Environment. Springer International Publishing, Cham, pp. 1–25. https://doi.org/10.1007/978-3-030-10618-8_48-1.

Fournier, E., Etienne-Mesmin, L., Grootaert, C., Jelsbak, L., Syberg, K., Blanquet-Diot, S., Mercier-Bonin, M., 2021a. Microplastics in the human digestive environment: afocus on the potential and challenges facing in vitro gut model development. J. Hazard. Mater. 415, 125632 https://doi.org/10.1016/j.jhazmat.2021.125632.

Fournier, E., Roussel, C., Dominicis, A., Ley, D., Peyron, M.-A., Collado, V., Mercier-Bonin, M., Lacroix, C., Alric, M., Van de Wiele, T., Chassard, C., Etienne-Mesmin, L., Blanquet-Diot, S., 2021b. In vitro models of gut digestion across childhood: current developments, challenges and future trends. Biotechnol. Adv., 107796 https://doi.org/10.1016/j.biotechadv.2021.107796.

Frias, J.P.G.L., Nash, R., 2019. Microplastics: finding a consensus on the definition. Mar. Pollut. Bull. 138, 145–147. https://doi.org/10.1016/j.marpolbul.2018.11.022.

Garner, C.E., Smith, S., de Lacy Costello, B., White, P., Spencer, R., Probert, C.S.J., Ratcliffem, N.M., 2007. Volatile organic compounds from feces and their potential for diagnosis of gastrointestinal disease. FASEB J. 21, 1675–1688. https://doi.org/10.1096/fj.06-6927com.

Gautam, R., Jo, J., Acharya, M., Maharjan, A., Lee, D., Pramod Bahadur, K.C., Kim, C., Kim, K., Kim, H., Heo, Y., 2022. Evaluation of potential toxicity of polyethylene microplastics on human derived cell lines. Sci. Total Environ., 156089 https://doi.org/10.1016/j.scitotenv.2022.156089.

Geirnaert, A., Calatayud, M., Grootaert, C., Laukens, D., Devriese, S., Smagghe, G., De Vos, M., Boon, N., Van, T., 2017. de Wiele, Butyrate-producing bacteria supplemented in vitro to Crohn's disease patient microbiota increased butyrate production and enhanced intestinal epithelial barrier integrity. Sci. Rep. 7, 11450. https://doi.org/10.1038/s41598-017-11734-8.

Giangeri, G., Morlino, M.S., De Bernardini, N., Ji, M., Bosaro, M., Pirillo, V., Antoniali, P., Molla, G., Raga, R., Treu, L., Campanaro, S., 2022. Preliminary investigation of microorganisms potentially involved in microplastics degradation using an integrated metagenomic and biochemical approach. Sci. Total Environ., 157017 https://doi.org/10.1016/j.scitotenv.2022.157017.

Gillois, K., Stoffels, C., Leveque, M., Fourquaux, I., Blesson, J., Mils, V., Cambier, S., Vignard, J., Terrisse, H., Mirey, G., Audinot, J.-N., Theodorou, V., Ropers, M.-H., Robert, H., Mercier-Bonin, M., 2021. Repeated exposure of Caco-2 versus Caco-2/HT29-MTX intestinal cell models to (nano)silver in vitro: comparison of two commercially available colloidal silver products. Sci. Total Environ. 754, 142324 https://doi.org/10.1016/j.scitotenv.2020.142324.

Hasani, A., Ebrahimzadeh, S., Hemmati, F., Khabbaz, A., Hasani, A., Gholizadeh, P., 2021. The role of Akkermansia muciniphila in obesity, diabetes and atherosclerosis. J. Med. Microbiol. 70 https://doi.org/10.1099/jmm.0.001435.

Henley, D.V., Bellone, C.J., Williams, D.A., Ruh, T.S., Ruh, M.F., 2004. Aryl hydrocarbon receptor-mediated posttranscriptional regulation of IL-1beta. Arch. Biochem Biophys. 422, 42–51. https://doi.org/10.1016/j.abb.2003.11.022.

Herter, C.A., 1908. The occurrence of skatol in the human intestine. J. Biol. Chem. 4, 101–109. https://doi.org/10.1016/S0021-9258(17)45972-2.

Hesler, M., Aengenheister, L., Ellinger, B., Drexel, R., Straskraba, S., Jost, C., Wagner, S., Meier, F., von Briesen, H., Büchel, C., Wick, P., Buerki-Thurnherr, T., Kohl, Y., 2019. Multi-endpoint toxicological assessment of polystyrene nano- and microparticles in different biological models in vitro. Toxicol. Vitr. 61, 104610 https://doi.org/10.1016/j.tiv.2019.104610.

Huang, D., Zhang, Y., Long, J., Yang, X., Bao, L., Yang, Z., Wu, B., Si, R., Zhao, W., Peng, C., Wang, A., Yan, D., 2022. Polystyrene microplastic exposure induces insulin resistance in mice via dysbacteriosis and pro-inflammation. Sci. Total Environ., 155937 https://doi.org/10.1016/j.scitotenv.2022.155937.

Hugenholtz, F., de Vos, W.M., 2018. Mouse models for human intestinal microbiota research: a critical evaluation. Cell Mol. Life Sci. 75, 149–160. https://doi.org/10.1007/s00018-017-2693-8.

Ibrahim, Y.S., Tuan Anuar, S., Azmi, A.A., Wan Mohd Khalik, W.M.A., Lehata, S., Hamzah, S.R., Ismail, D., Ma, Z.F., Dzulkarnaen, A., Zakaria, Z., Mustaffa, N., Tuan Sharif, S.E., Lee, Y.Y., 2021. Detection of microplastics in human colectomy specimens. JGH Open 5, 116–121. https://doi.org/10.1002/jgh3.12457.

Jin, Y., Lu, L., Tu, W., Luo, T., Fu, Z., 2019. Impacts of polystyrene microplastic on the gut barrier, microbiota and metabolism of mice. Sci. Total Environ. 649, 308–317. https://doi.org/10.1016/j.scitotenv.2018.08.353.

Kalantar-Zadeh, K., Berean, K.J., Burgell, R.E., Muir, J.G., Gibson, P.R., 2019. Intestinal gases: influence on gut disorders and the role of dietary manipulations. Nat. Rev. Gastroenterol. Hepatol. 16, 733–747. https://doi.org/10.1038/s41575-019-0193-z.

Lamas, B., Richard, M.L., Leducq, V., Pham, H.-P., Michel, M.-L., Da Costa, G., Bridonneau, C., Jegou, S., Hoffmann, T.W., Natividad, J.M., Brot, L., Taleb, S., Couturier-Maillard, A., Nion-Larmurier, I., Merabtene, F., Seksik, P., Bourrier, A., Cosnes, J., Ryffel, B., Beaugerie, L., Launay, J.-M., Langella, P., Xavier, R.J., Sokol, H., 2016. CARD9 impacts colitis by altering gut microbiota metabolism of tryptophan into aryl hydrocarbon receptor ligands. Nat. Med 22, 598–605. https://doi.org/10.1038/nm.4102.

Lamas, B., Natividad, J.M., Sokol, H., 2018. Aryl hydrocarbon receptor and intestinal immunity. Mucosal Immunol. 11, 1024–1038. https://doi.org/10.1038/s41385-018-0019-2.

Lamas, B., Hernandez-Galan, L., Galipeau, H.J., Constante, M., Clarizio, A., Jury, J., Breyner, N.M., Caminero, A., Rueda, G., Hayes, C.L., McCarville, J.L., Bermudez Brito, M., Planchais, J., Rolhion, N., Murray, J.A., Langella, P., Loonen, L.M.P., Wells, J.M., Bercik, P., Sokol, H., Verdu, E.F., 2020. Aryl hydrocarbon receptor ligand production by the gut microbiota is decreased in celiac disease leading to intestinal inflammation. eaba0624 Sci. Transl. Med. 12. https://doi.org/10.1126/scitranslmed.aba0624.

Lehel, J., Murphy, S., 2021. Microplastics in the food chain: food safety and environmental aspects. Rev. Environ. Contam. Toxicol. 259, 1–49. https://doi.org/10.1007/398_2021_77.

Lemfack, M.C., Nickel, J., Dunkel, M., Preissner, R., Piechulla, B., 2014. mVOC: a database of microbial volatiles. Nucleic Acids Res. 42, D744–D748. https://doi.org/10.1093/nar/gkt1250.

Leslie, H.A., van Velzen, M.J.M., Brandsma, S.H., Vethaak, A.D., Garcia-Vallejo, J.J., Lamoree, M.H., 2022. Discovery and quantification of plastic particle pollution in human blood. Environ. Int., 107199 https://doi.org/10.1016/j.envint.2022.107199.

Li, B., Ding, Y., Cheng, X., Sheng, D., Xu, Z., Rong, Q., Wu, Y., Zhao, H., Ji, X., Zhang, Y., 2020. Polyethylene microplastics affect the distribution of gut microbiota and inflammation development in mice. Chemosphere 244, 125492. https://doi.org/10.1016/j.chemosphere.2019.125492.

Lindell, A.E., Zimmermann-Kogadeeva, M., Patil, K.R., 2022. Multimodal interactions of drugs, natural compounds and pollutants with the gut microbiota. Nat. Rev. Microbiol 20, 431–443. https://doi.org/10.1038/s41579-022-00681-5.

Liu, P., Zhan, X., Wu, X., Li, J., Wang, H., Gao, S., 2019. Effect of weathering on environmental behavior of microplastics: Properties, sorption and potential risks. Chemosphere 242, 125193. https://doi.org/10.1016/j.chemosphere.2019.125193.

Liu, S., Wu, X., Gu, W., Yu, J., Wu, B., 2020a. Influence of the digestive process on intestinal toxicity of polystyrene microplastics as determined by in vitro Caco-2 models. Chemosphere 256, 127204. https://doi.org/10.1016/j.chemosphere.2020.127204.

Liu, W., Zhang, R., Shu, R., Yu, J., Li, H., Long, H., Jin, S., Li, S., Hu, Q., Yao, F., Zhou, C., Huang, Q., Hu, X., Chen, M., Hu, W., Wang, Q., Fang, S., Wu, Q., 2020b. Study of the relationship between microbiome and colorectal cancer susceptibility using 16SrRNA sequencing. Biomed. Res. Int. 2020, 7828392 https://doi.org/10.1155/2020/7828392.

Lu, L., Wan, Z., Luo, T., Fu, Z., Jin, Y., 2018. Polystyrene microplastics induce gut microbiota dysbiosis and hepatic lipid metabolism disorder in mice. Sci. Total Environ. 631– 632, 449–458. https://doi.org/10.1016/j.scitotenv.2018.03.051.

Morrison, D.J., Preston, T., 2016. Formation of short chain fatty acids by the gut microbiota and their impact on human metabolism. Gut Microbes 7, 189–200. https://doi.org/10.1080/19490976.2015.1134082.

Murali, A., Bhargava, A., Wright, E.S., 2018. IDTAXA: a novel approach for accurate taxonomic classification of microbiome sequences. Microbiome 6, 140. https://doi.org/10.1186/s40168-018-0521-5.

Natividad, J.M., Agus, A., Planchais, J., Lamas, B., Jarry, A.C., Martin, R., Michel, M.-L., Chong-Nguyen, C., Roussel, R., Straube, M., Jegou, S., McQuitty, C., Le Gall, M., da Costa, G., Lecornet, E., Michaudel, C., Modoux, M., Glodt, J., Bridonneau, C., Sovran, B., Dupraz, L., Bado, A., Richard, M.L., Langella, P., Hansel, B., Launay, J.-M., Xavier, R.J., Duboc, H., Sokol, H., 2018. Impaired aryl hydrocarbon receptor ligand production by the gut microbiota is a key factor in metabolic syndrome. e4 Cell Metab. 28, 737–749. https://doi.org/10.1016/j.cmet.2018.07.001.

Oksanen, J., Blanchet, F.G., Kindt, R., Legendre, P., O'Hara, R., Simpson, G., Solymos, P., Stevens, H., Wagner, H., 2011. Vegan: community ecology package. R. Package Version 1, 17–18.

Parks, D.H., Chuvochina, M., Rinke, C., Mussig, A.J., Chaumeil, P.-A., Hugenholtz, P., 2022. GTDB: an ongoing census of bacterial and archaeal diversity through a

phylogenetically consistent, rank normalized and complete genome-based taxonomy. Nucleic Acids Res. 50, D785–D794. https://doi.org/10.1093/nar/gkab776.
Pei, X.-H., Nakanishi, Y., Inoue, H., Takayama, K., Bai, F., Hara, N., 2002. Polycyclic aromatic hydrocarbons induce IL-8 expression through nuclear factor kappaB activation in A549 cell line. Cytokine 19, 236–241. https://doi.org/10.1006/cyto.2002.1967.
Pelaseyed, T., Bergström, J.H., Gustafsson, J.K., Ermund, A., Birchenough, G.M.H., Schütte, A., van der Post, S., Svensson, F., Rodríguez-Piñeiro, A.M., Nyström, E.E.L., Wising, C., Johansson, M.E.V., Hansson, G.C., 2014. The mucus and mucins of the goblet cells and enterocytes provide the first defense line of the gastrointestinal tract and interact with the immune system. Immunol. Rev. 260, 8–20. https://doi.org/10.1111/imr.12182.
Pittayanon, R., Lau, J.T., Yuan, Y., Leontiadis, G.I., Tse, F., Surette, M., Moayyedi, P., 2019. Gut microbiota in patients with irritable bowel syndrome-a systematic review. Gastroenterology. https://doi.org/10.1053/j.gastro.2019.03.049.
Prescott, M.J., Lidster, K., 2017. Improving quality of science through better animal welfare: the NC3Rs strategy. Lab Anim. (NY). 46, 152–156. https://doi.org/10.1038/laban.1217.
Provencher, J.F., Covernton, G.A., Moore, R.C., Horn, D.A., Conkle, J.L., Lusher, A.L., 2020. Proceed with caution: the need to raise the publication bar for microplastics research. Sci. Total Environ. 748, 141426 https://doi.org/10.1016/j.scitotenv.2020.141426.
Quast, C., Pruesse, E., Yilmaz, P., Gerken, J., Schweer, T., Yarza, P., Peplies, J., Glöckner, F.O., 2013. The SILVA ribosomal RNA gene database project: improved data processing and web-based tools. Nucleic Acids Res. 41, D590–D596. https://doi.org/10.1093/nar/gks1219.
Raman, M., Ahmed, I., Gillevet, P.M., Probert, C.S., Ratcliffe, N.M., Smith, S., Greenwood, R., Sikaroodi, M., Lam, V., Crotty, P., Bailey, J., Myers, R.P., Rioux, K.P., 2013. Fecal microbiome and volatile organic compound metabolome in obese humans with nonalcoholic fatty liver disease. e3 Clin. Gastroenterol. Hepatol. 11, 868–875. https://doi.org/10.1016/j.cgh.2013.02.015.
E. Rifa, S. Theil, ExploreMetabar: v1.0.0, (2021). https://doi.org/10.5281/ZENODO.5245195.
Roager, H.M., Licht, T.R., 2018. Microbial tryptophan catabolites in health and disease. Nat. Commun. 9, 3294. https://doi.org/10.1038/s41467-018-05470-4.
Rooks, M.G., Garrett, W.S., 2016. Gut microbiota, metabolites and host immunity. Nat. Rev. Immunol. 16, 341–352. https://doi.org/10.1038/nri.2016.42.
Rothhammer, V., Quintana, F.J., 2019. The aryl hydrocarbon receptor: an environmental sensor integrating immune responses in health and disease. Nat. Rev. Immunol. 19, 184–197. https://doi.org/10.1038/s41577-019-0125-8.
Schenkel, D., Lemfack, M.C., Piechulla, B., Splivallo, R., 2015. A meta-analysis approach for assessing the diversity and specificity of belowground root and microbial volatiles. Front Plant Sci. 6, 707. https://doi.org/10.3389/fpls.2015.00707.
Schliep, K., Potts, A.J., Morrison, D.A., Grimm, G.W., 2017. Intertwining phylogenetic trees and networks. Methods Ecol. Evol. 8, 1212–1220. https://doi.org/10.1111/2041-210X.12760.
Schwabl, P., Köppel, S., Königshofer, P., Bucsics, T., Trauner, M., Reiberger, T., Liebmann, B., 2019. Detection of various microplastics in human stool: a prospective case series. Ann. Intern. Med. 171, 453–457. https://doi.org/10.7326/M19-0618.
Senathirajah, K., Attwood, S., Bhagwat, G., Carbery, M., Wilson, S., Palanisami, T., 2021. Estimation of the mass of microplastics ingested - a pivotal first step towards human health risk assessment. J. Hazard Mater. 404, 124004 https://doi.org/10.1016/j.jhazmat.2020.124004.
Shi, J., Zhao, D., Song, S., Zhang, M., Zamaratskaia, G., Xu, X., Zhou, G., Li, C., 2020. High-meat-protein high-fat diet induced dysbiosis of gut microbiota and tryptophan metabolism in wistar rats. J. Agric. Food Chem. 68, 6333–6346. https://doi.org/10.1021/acs.jafc.0c00245.
Smith, E.A., Macfarlane, G.T., 1997. Formation of phenolic and indolic compounds by anaerobic bacteria in the human large intestine. Micro Ecol. 33, 180–188. https://doi.org/10.1007/s002489900020.
Stange, E.F., Schroeder, B.O., 2019. Microbiota and mucosal defense in IBD: an update. Expert Rev. Gastroenterol. Hepatol. 13, 963–976. https://doi.org/10.1080/17474124.2019.1671822.
Stock, V., Fahrenson, C., Thuenemann, A., Dönmez, M.H., Voss, L., Böhmert, L., Braeuning, A., Lampen, A., Sieg, H., 2019. Impact of artificial digestion on the sizes and shapes of microplastic particles. Food Chem. Toxicol., 111010 https://doi.org/10.1016/j.fct.2019.111010.
Stock, V., Böhmert, L., Coban, G., Tyra, G., Vollbrecht, M.-L., Voss, L., Paul, M.B., Braeuning, A., Sieg, H., 2022. Microplastics and nanoplastics: size, surface and dispersant - What causes the effect? Toxicol. Vitr., 105314 https://doi.org/10.1016/j.tiv.2022.105314.
Su, L., Xiong, X., Zhang, Y., Wu, C., Xu, X., Sun, C., Shi, H., 2022. Global transportation of plastics and microplastics: a critical review of pathways and influences. Sci. Total Environ., 154884 https://doi.org/10.1016/j.scitotenv.2022.154884.
Sun, H., Chen, N., Yang, X., Xia, Y., Wu, D., 2021. Effects induced by polyethylene microplastics oral exposure on colon mucin release, inflammation, gut microflora composition and metabolism in mice. Ecotoxicol. Environ. Saf. 220, 112340 https://doi.org/10.1016/j.ecoenv.2021.112340.
Suyama, Y., Hirayama, C., 1988. Serum indole and skatole in patients with various liver diseases. Clin. Chim. Acta 176, 203–206. https://doi.org/10.1016/0009-8981(88)90208-2.
Tamaki, A., Hayashi, H., Nakajima, H., Takii, T., Katagiri, D., Miyazawa, K., Hirose, K., Onozaki, K., 2004. Polycyclic aromatic hydrocarbon increases mRNA level for interleukin 1 beta in human fibroblast-like synoviocyte line via aryl hydrocarbon receptor. Biol. Pharm. Bull. 27, 407–410. https://doi.org/10.1248/bpb.27.407.
Tamargo, A., Molinero, N., Reinosa, J.J., Alcolea-Rodriguez, V., Portela, R., Bañares, M. A., Fernández, J.F., Moreno-Arribas, M.V., 2022. PET microplastics affect human gut microbiota communities during simulated gastrointestinal digestion, first evidence of plausible polymer biodegradation during human digestion. Sci. Rep. 12, 528. https://doi.org/10.1038/s41598-021-04489-w.
Tang, A., Bi, X., Du, J., Rao, L., Vasanthakumar, V., Hu, Y.-B., Fu, M.-L., Sun, W., Yuan, B., 2022. The effect of polyethylene microplastics on the disinfection of Escherichia coli by sodium hypochlorite. Sci. Total Environ., 155322 https://doi.org/10.1016/j.scitotenv.2022.155322.
Tareen, A., Saeed, S., Iqbal, A., Batool, R., Jamil, N., 2022. Biodeterioration of microplastics: a promising step towards plastics waste management. Polymers (Basel) 14, 2275. https://doi.org/10.3390/polym14112275.
Theil, S., Rifa, E., 2021. rANOMALY: amplicon workflow for microbial community analysis. F1000Res 10, 7. https://doi.org/10.12688/f1000research.27268.1.
Thévenot, J., Cordonnier, C., Rougeron, A., Le Goff, O., Nguyen, H.T.T., Denis, S., Alric, M., Livrelli, V., Blanquet-Diot, S., 2015. Enterohemorrhagic Escherichia coli infection has donor-dependent effect on human gut microbiota and may be antagonized by probiotic yeast during interaction with Peyer's patches. Appl. Microbiol Biotechnol. 99, 9097–9110. https://doi.org/10.1007/s00253-015-6704-0.
Thursby, E., Juge, N., 2017. Introduction to the human gut microbiota. Biochem. J. 474, 1823–1836. https://doi.org/10.1042/BCJ20160510.
Tu, C., Chen, T., Zhou, Q., Liu, Y., Wei, J., Waniek, J.J., Luo, Y., 2020. Biofilm formation and its influences on the properties of microplastics as affected by exposure time and depth in the seawater. Sci. Total Environ. 734, 139237 https://doi.org/10.1016/j.scitotenv.2020.139237.
Vyhlídalová, B., Krasulová, K., Pečinková, P., Marcalíková, A., Vrzal, R., Zemánková, L., Vančo, J., Trávníček, Z., Vondráček, J., Karasová, M., Mani, S., Dvořák, Z., 2020. Gut microbial catabolites of tryptophan are ligands and agonists of the aryl hydrocarbon receptor: a detailed characterization. Int J. Mol. Sci. 21, E2614 https://doi.org/10.3390/ijms21072614.
Walton, C., Fowler, D.P., Turner, C., Jia, W., Whitehead, R.N., Griffiths, L., Dawson, C., Waring, R.H., Ramsden, D.B., Cole, J.A., Cauchi, M., Bessant, C., Hunter, J.O., 2013. Analysis of volatile organic compounds of bacterial origin in chronic gastrointestinal diseases. Inflamm. Bowel Dis. 19, 2069–2078. https://doi.org/10.1097/MIB.0b013e31829a91f6.
Wang, L., Wu, W.-M., Bolan, N.S., Tsang, D.C.W., Li, Y., Qin, M., Hou, D., 2021. Environmental fate, toxicity and risk management strategies of nanoplastics in the environment: current status and future perspectives. J. Hazard. Mater. 401, 123415 https://doi.org/10.1016/j.jhazmat.2020.123415.
Waters, J.L., Ley, R.E., 2019. The human gut bacteria Christensenellaceae are widespread, heritable, and associated with health. BMC Biol. 17, 83. https://doi.org/10.1186/s12915-019-0699-4.
Wen, S., Zhao, Y., Liu, S., Chen, Y., Yuan, H., Xu, H., 2022. Polystyrene microplastics exacerbated liver injury from cyclophosphamide in mice: insight into gut microbiota. Sci. Total Environ., 156668 https://doi.org/10.1016/j.scitotenv.2022.156668.
Yan, Z., Liu, Y., Zhang, T., Zhang, F., Ren, H., Zhang, Y., 2022. Analysis of microplastics in human feces reveals a correlation between fecal microplastics and inflammatory bowel disease status. Environ. Sci. Technol. 56, 414–421. https://doi.org/10.1021/acs.est.1c03924.
Yokoyama, M.T., Carlson, J.R., 1979. Microbial metabolites of tryptophan in the intestinal tract with special reference to skatole. Am. J. Clin. Nutr. 32, 173–178. https://doi.org/10.1093/ajcn/32.1.173.
Yu, F., Yang, C., Zhu, Z., Bai, X., Ma, J., 2019. Adsorption behavior of organic pollutants and metals on micro/nanoplastics in the aquatic environment. Sci. Total Environ. 694, 133643 https://doi.org/10.1016/j.scitotenv.2019.133643.
Yu, Y., Lee, C., Kim, J., Hwang, S., 2005. Group-specific primer and probe sets to detect methanogenic communities using quantitative real-time polymerase chain reaction. Biotechnol. Bioeng. 89, 670–679. https://doi.org/10.1002/bit.20347.
Zettler, E.R., Mincer, T.J., Amaral-Zettler, L.A., 2013. Life in the "Plastisphere": microbial communities on plastic marine debris. Environ. Sci. Technol. 47, 7137–7146. https://doi.org/10.1021/es401288x.
Zhang, J., Wang, L., Trasande, L., Kannan, K., 2021a. Occurrence of polyethylene terephthalate and polycarbonate microplastics in infant and adult feces. Environ. Sci. Technol. Lett. 8, 989–994. https://doi.org/10.1021/acs.estlett.1c00559.
Zhang, K., Hamidian, A.H., Tubić, A., Zhang, Y., Fang, J.K.H., Wu, C., Lam, P.K.S., 2021a. Understanding plastic degradation and microplastic formation in the environment: a review. Environ. Pollut. 274, 116554 https://doi.org/10.1016/j.envpol.2021.116554.
Zhang, N., Li, Y.B., He, H.R., Zhang, J.F., Ma, G.S., 2021a. You are what you eat: Microplastics in the feces of young men living in Beijing. Sci. Total Environ. 767, 144345 https://doi.org/10.1016/j.scitotenv.2020.144345.
Zhang, X., Coker, O.O., Chu, E.S., Fu, K., Lau, H.C.H., Wang, Y.-X., Chan, A.W.H., Wei, H., Yang, X., Sung, J.J.Y., Yu, J., 2021c. Dietary cholesterol drives fatty liver-associated liver cancer by modulating gut microbiota and metabolites. Gut 70, 761–774. https://doi.org/10.1136/gutjnl-2019-319664.
Zhang, Y., Wang, S., Olga, V., Xue, Y., Lv, S., Diao, X., Zhang, Y., Han, Q., Zhou, H., 2021b. The potential effects of microplastic pollution on human digestive tract cells. Chemosphere, 132714. https://doi.org/10.1016/j.chemosphere.2021.132714.
Zhu, W., Winter, M.G., Byndloss, M.X., Spiga, L., Duerkop, B.A., Hughes, E.R., Büttner, L., de Lima Romão, E., Behrendt, C.L., Lopez, C.A., Sifuentes-Dominguez, L., Huff-Hardy, K., Wilson, R.P., Gillis, C.C., Tükel, Ç., Koh, A.Y., Burstein, E., Hooper, L.V., Bäumler, A.J., Winter, S.E., 2018. Precision editing of the gut microbiota ameliorates colitis. Nature 553, 208–211. https://doi.org/10.1038/nature25172.